

Allosteric control of an asymmetric transduction in a G protein-coupled receptor heterodimer

Junke Liu^{1,*}, Zongyong Zhang^{1,*}, David Moreno-Delgado², James A.R. Dalton⁴, Xavier Rovira², Ana Trapero³, Cyril Goudet², Amadeu Llebaria³, Jesus Giraldo⁴, Qilin Yuan¹, Philippe Rondard^{2,3*}, Siluo Huang^{1#,+}, Jianfeng Liu^{1#,+}, Jean-Philippe Pin^{2#,+}

¹ Sino-France Laboratory of cellular signaling, Key Laboratory of Molecular Biophysics of Ministry of Education, College of Life Science and Technology and Collaborative Innovation Center for Genetics and Development, Huazhong University of Science and Technology, Wuhan, Hubei, China;

² Institut de Génomique Fonctionnelle (IGF), CNRS, INSERM, Univ. Montpellier, F-34000 Montpellier, France;

³ MCS, Laboratory of Medicinal Chemistry & Synthesis, Institute for Advanced Chemistry of Catalonia (IQAC-CSIC), Barcelona, Spain.

⁴ Institut de Neurociències and Unitat de Bioestadística, Universitat Autònoma de Barcelona (UAB), and Network Biomedical Research Center on Mental Health (CIBERSAM), Barcelona, Spain

[#]To whom correspondence should be addressed: Huang SL (slhuang@mail.hust.edu.cn), Liu JF (jfliu@mail.hust.edu.cn) or Pin JP. (jppin@igf.cnrs.fr)

^{*,+,}: these authors contributed equally to this work

Running title: Allosteric signaling of mGlu heterodimer.

Abstract

GPCRs play critical roles in cell communication. Although GPCRs can form heteromers, their role in signaling remains elusive. Here we used rat metabotropic glutamate (mGlu) receptors as prototypical dimers to study the functional interaction between each subunit. mGluRs can form both constitutive homo- and heterodimers. Whereas both mGlu2 and mGlu4 couple to G proteins, G protein activation is mediated by mGlu4 heptahelical domain (HD) exclusively in mGlu2-4 heterodimers. Such asymmetric transduction results from the action of both the dimeric extracellular domain, and an allosteric activation by the partially-activated non-functional mGlu2 HD. G proteins activation by mGlu2 HD occurs if either the mGlu2 HD is occupied by a positive allosteric modulator or if mGlu4 HD is inhibited by a negative modulator. These data revealed an oriented asymmetry in mGlu heterodimers that can be controlled with allosteric modulators. They provide new insight on the allosteric interaction between subunits in a GPCR dimer.

One sentence summary

In mGlu heterodimers, an oriented asymmetrical activation revealed complex allosteric interaction between subunits

Introduction

Many cell surface receptors form multi-protein complexes for signaling integration (1-4). Among them, G protein-coupled receptors (GPCRs) are the most abundant and constitute the main targets in drug development (5). Although most GPCRs can signal in a monomeric form (6-8), increasing studies revealed that they can associate into both homo and heteromeric complexes (9-13). Interestingly, GPCR heteromers may generate original functional pharmacological entities different from each of the homomers (10, 11, 14-17). Whether such GPCR association is real in native tissue is still a matter of intense debate (18, 19). Understanding how a receptor can control the activity of its partner (4, 13, 16, 20, 21) will certainly help clarify this important issue, opening ways to control the function of GPCR heteromers.

Metabotropic glutamate receptors (mGluRs) are class C GPCRs and are well-recognized constitutive homodimers (22, 23). These receptors are divided into three groups: group I (mGlu_{1,5}), II (mGlu_{2,3}) and III (mGlu_{4,6,7,8}), on the basis of sequence homology, pharmacological profile and cellular signaling. Recently, mGluRs were shown to also form heterodimers with specific subunit composition (24, 25). Of note, whereas the different mGluRs were commonly described as having specific brain distribution supporting their homodimeric nature, localization studies revealed subcellular co-localization of different mGluRs such as mGlu1 and 5 (26), mGlu2 and 4 (27), mGlu7 and 8 (28). Further studies supported the existence of mGlu2-4 and 1-5 heterodimers in the brain (26, 27, 29). Being identified very recently, not much is known about the possible clinical relevance of mGlu heterodimers, but already homodimeric mGlu4, rather than heterodimeric mGlu2-4, were proposed as a better target for Parkinson's disease treatment (30). In contrast, mGlu2-4 heterodimers control synaptic activity at the level of the cortico-striatal terminals in the striatum (27) and lateral perforant path terminals in the dentate gyrus (29).

The mGlu subunits are multidomain proteins composed of a Venus flytrap domain (VFT) containing the orthosteric binding site, connected via a cysteine-rich domain (CRD) to a heptahelical domain (HD) involved in G protein coupling (23, 31-34). In the case of mGlu homodimers, structural and biophysical studies revealed a symmetrical conformational

change during activation at the level of the VFTs (35-40). Indeed, while activating one VFT is sufficient to partially activate the homodimers, activating both VFTs is required for full activity both in homodimeric (41-43) and heterodimeric receptors (29). Surprisingly, this symmetric activation of the VFT dimer leads to an asymmetric activation of the HD dimer, only one HD being active at a time (44-46). Whether mGlu heterodimer activation is symmetric or asymmetric, and whether either subunit can be involved in signaling remains unknown. Such analysis will likely bring interesting observation for the understanding of the allosteric coupling between GPCRs within hetero-complexes.

In this study, we choose mGlu2-4 heterodimer as a prototype heterodimer, as its existence in the brain has been documented (27, 29). We show that whereas both mGlu2 and mGlu4 HDs are capable of activating G proteins, only mGlu4 HD does it in mGlu2-4 heterodimers. Although a conformational change in the mGlu2 HD occurs that can be prevented by a mGlu2 negative allosteric modulator (NAM), it is not sufficient for a direct activation of G proteins, but important for the G protein coupling by the associated mGlu4 HD. This further documents the asymmetric activation of dimeric GPCRs. Furthermore, we demonstrated that manipulating the conformation of either mGlu2 or mGlu4 HD with positive and negative allosteric modulators can reorient the asymmetry towards mGlu2 activating G proteins. This demonstrates a differential ability of mGlu2 and mGlu4 HD to reach a G protein activating state. But most importantly, these data reveal strong allosteric interactions between two GPCRs in a dimeric complex. Such allosteric coupling can be controlled with small molecules revealing a way to modulate heteromeric receptor activity, and expanding the possibilities of using such small molecules to precisely control signaling events. This illustrates how such hetero-complexes can control signals originating from various GPCR ligands targeting a cell.

99 **Results**

100 **mGlu2-4 heterodimer activates G protein through mGlu4**

101 The difficulty in studying GPCR heterodimers is that the co-expression of two different
102 receptors leads to three populations of dimers, both homodimers and the heterodimer, making
103 difficult the study of the specific properties of the heterodimeric entity. We then used a quality
104 control system that allows cell surface targeting of the heterodimer only (42). We engineered
105 chimeric mGlu2 and mGlu4 subunits containing complementary coiled-coil regions (C1 and
106 C2) derived from the GABA_B receptor and intracellular retention signals (KKXX) (37, 41).
107 We constructed mGlu2 and mGlu4 mutants with either C1 or C2, such as ^{HA}mGlu2_{C1KKXX}
108 (2_{C1}), ^{Flag}mGlu2_{C2KKXX} (2_{C2}), ^{HA}mGlu4_{C1KKXX} (4_{C1}) and ^{Flag}mGlu4_{C2KKXX} (4_{C2}). By combination
109 of C1 and C2 containing subunits, we can obtain the mGlu2-4 heterodimers specifically at the
110 cell surface, as well as the mGlu2 (2-2) and mGlu4 (4-4) homodimers as controls (Figure
111 1A,B).

112 Such receptor constructs retained their ability to activate G proteins (we used the chimeric
113 Gqi and Gqo proteins that enable coupling of these receptors to the PLC pathway (47, 48))
114 when at the cell surface, with the expected action of mGlu2 (DCG-IV) and mGlu4 (L-AP4)
115 selective agonists (Figure 1-figure supplement 1). When activated with glutamate, mGlu2 and
116 mGlu2-4 displayed a similar potency and efficacy, while glutamate had a lower efficacy at
117 mGlu4 (Figure 1C, Figure 1-source data file 1). Note that all these receptor combinations
118 were expressed at a similar level at the cell surface (Figure 1B).

119 Mutating the conserved Phe residue into Ser in the third intracellular loop of mGluRs
120 abolished their ability to activate G proteins (41, 45). When introduced into the C1 and C2
121 constructs, neither mGlu2-F756S, nor mGlu4-F781S activated G proteins (Figure 1D,E).
122 When only one subunit carries the mutation, a larger decrease in glutamate efficacy was
123 observed in mGlu2 dimers than in mGlu4 dimers (Figure 1D,E, Figure 1-figure 1 source data
124 file 1). When such mutation was introduced in the mGlu2 subunit of the mGlu2-4 heterodimer,
125 a glutamate-mediated response similar to the control was observed (Figure 1D,F, Figure
126 1-source data file 1). In contrast, in the heterodimer containing the mutated mGlu4 subunit no
127 response could be observed (Figure 1F) despite a correct expression level at the cell surface

(Figure 1-figure supplement 2). As a control, introducing the FS mutation in both subunits of mGlu2-4 heterodimer abolished glutamate-induced G protein signaling (Figure 1-figure supplement 3A). Even when the selective mGlu2 and mGlu4 agonists DCG-IV and L-AP4 were used, signal could be generated with the heterodimers mutated in the mGlu2 subunit, but not in those mutated in the mGlu4 subunits (Figure 1-figure supplement 3B-D). Such data strongly suggest that in the heterodimer, G protein activation is exclusively mediated by mGlu4 HD. Of note, similar results were obtained with either mGlu2_{C1-4C2} or 4_{C1-2C2} heterodimers, indicating that the modified C terminal domains do not influence the asymmetric activation (Figure 1C, F).

Asymmetric activation of mGlu2-4 HDs relies on the HDs only

In order to understand how a symmetric mGlu2-4 activation at the level of the VFT dimer could control an asymmetric activation of the HD dimer, we examined whether this could result from the specific association of one HD with its extracellular domain (ECD, composed of the VFT and the CRD). We then generated various constructs leading to the surface expression of receptor combinations composed of a 2-4 heterodimeric HD, but carrying either two mGlu2 ECDs (2-2^{ECD}4^{HD}; Figure 2A), two mGlu4 ECDs (4-4^{ECD}2^{HD}; Figure 2B), or in which the ECDs were swapped between the two subunits (2^{ECD}4^{HD}-4^{ECD}2^{HD}; Figure 2C). Constructs leading to the receptor combinations containing two mGlu2 VFTs (Figure 2-figure supplement 1A), two mGlu4 VFTs (Figure 2-figure supplement 1B), or in which the VFTs were swapped between the two subunits (Figure 2-figure supplement 1C) were also generated. For any of these combinations, we also analyzed the functional consequence of mutating either the mGlu2 or mGlu4 HD (Figure 2 and Figure 2-figure supplement 1). Thanks to the C1 C2 terminal tails, a correct and specific expression of any of the indicated dimer combinations at the cell surface could be verified thanks to the HA or Flag N-terminal epitopes (Figure 2-figure supplement 2 and 3).

When activated by glutamate, we found that any combination carrying a wild-type mGlu4 HD (with or without a mutated mGlu2 HD) generated Ca²⁺ signals (Figure 2 and Figure 2-figure supplement 1). In contrast, none of those carrying a mutated mGlu4 HD were functional (Figure 2 and Figure 2-figure supplement 1) despite their expression at the cell

surface (Figure 2-figure supplement 2 and 3). Similarly, activating specifically the mGlu2 VFT with DCG-IV, or the mGlu4 VFT with L-AP4 led to G protein signaling of receptor combinations carrying at least one mGlu2 VFT, or one mGlu4 VFT, respectively, as long as the receptor contained a wild-type mGlu4 HD. No response could be generated with these agonists in receptor combinations carrying a mutated mGlu4 HD (Figure 2 and Figure 2-figure supplement 1).

We then examined the functional consequence of locking the ECD dimer in its active orientation. We previously reported that an inter-subunit disulfide bond between a Cys introduced at position 521 of the mGlu2 CRD led to a fully active dimer (mGlu2^C) (37). Mutating the equivalent position in mGlu4 (His523Cys) also generated a fully active receptor (mGlu4^C) (Figure 3A), as revealed by the accumulation of inositol monophosphate after LiCl addition. Note that the constitutive activation of phospholipase C cannot be quantified through intracellular Ca²⁺ measurements because Ca²⁺ concentrations return close to basal values under constant PLC activity. When both mGlu2^C and mGlu4^C were co-expressed, an inter-subunit DTT-sensitive covalent linkage could be demonstrated, providing the natural inter-VFT disulfide bond is mutated (Figure 3B). Such a receptor combination also displayed a full constitutive activity (Figure 3A). In that case again, the high constitutive or glutamate-induced signaling could be observed in the heterodimer combinations containing a wild-type mGlu4 HD but not in those in which the mGlu4 HD contained the FS mutation (Figure 3A) despite a correct expression of all constructs (Figure 3-figure supplement 1)

Taken together, these results demonstrate that any ways the dimeric ECD of the mGlu2-4 heterodimer is activated the mGlu4 HD is always responsible for G protein activation. This strongly suggests that the asymmetric activity of the mGlu2-4 HD dimer is an intrinsic property of this membrane part of the receptor.

mGlu2 HD is involved in the activation of mGlu4 HD

Although mGlu2 HD is not directly responsible for G protein activation in the mGlu2-4 heterodimer, it may still play a role in the activation process. We then used MNI137, an mGlu2 NAM (49) known to stabilize the mGlu2 HD in its inactive conformation. We found that MNI137 partially inhibited mGlu2-4 heterodimer while it largely inhibited the response

of the mGlu2 homodimer, whether the dimer was activated by glutamate (Figure 4A, Figure 4-source data file 1) or was constitutively active through the inter-CRD disulfide bridge (Figure 4B, Figure 4-source data file 2). Of note, similar data were obtained in a receptor combination in which the mGlu2 subunit is incapable of G protein coupling. This revealed that a conformational change in the mGlu2 HD prevented by MNI137 binding is required to fully activate the mGlu4 HD.

To clarify how mGlu2 HD in the heterodimer controls mGlu4 HD activation, we activated the heterodimer with specific agonist of either mGlu2 or mGlu4. Interestingly, we found that MNI137 blocked mGlu2-4 heterodimer signaling induced by either DCG-IV or L-AP4 respectively whereas MNI137 inhibited only partially signaling induced by the combination of DCG IV and L-AP4 as observed with glutamate (Figure 4A,C, Figure 4-source data file 3). These data revealed the prominent role of mGlu2 HD in activating mGlu4 HD when only one VFT is activated. Consistent with this conclusion, activation of both VFTs with DCG-IV in receptor combinations containing two mGlu2 VFTs is only partially inhibited by MNI137, with a smaller inhibition ($39.2 \pm 4.7\%$, $n=3$) when both CRDs are from mGlu2, compared to the situation where the mGlu4 HD is associated with the mGlu4 CRD ($64.3 \pm 3.8\%$ inhibition, $n=3$, $p<0.05$) (Figure 4D).

Allosteric control of the asymmetric activation of mGlu2-4 HDs

We then examined why mGlu2 HD could not mediate G protein activation within the mGlu2-4 heterodimer. We first analyzed the effect of an mGlu4 NAM (OptoGluNAM4.1) that we recently reported to prevent mGlu4 HD activation (50). Surprisingly, this compound, while inhibiting agonist-mediated mGlu4 activity (50), had no effect on the mGlu2-4 heterodimer (Figure 5A). Most interestingly, when using an mGlu2-4 combination in which the mGlu4 HD is unable to activate G protein, then a heterodimer unable to activate G proteins, the addition of OptoGluNAM4.1 allowed glutamate to generate a signal (Figure 5A, Figure 5-source data file 1). This suggests that, by preventing mGlu4 HD to reach its active state, mGlu2 HD can take over for G protein activation in the heterodimer.

Such a proposal is supported by a second set of experiments, in which we favored mGlu2 HD activation in the mGlu2-4 heterodimer using the mGlu2 PAM LY487379. This compound

had no significant effect on the mGlu2-4 heterodimer signaling capacity (Figure 5B, Figure 5-source data file 1) or on the mGlu2-4 heterodimer mutated in mGlu2 HD (Figure 5-source data file 1). However, on the non-functional mGlu2-4 combination where the mGlu4 HD is mutated, the mGlu2 PAM LY487379 allowed glutamate to activate G proteins, therefore revealing a possible coupling of the mGlu2 HD in this heterodimer.

Taken together, these data revealed that under normal conditions, the coupling of mGlu2-4 is mediated by mGlu4 HD, but the mGlu2 HD can still generate signaling providing its activation is facilitated by a PAM, or by the inhibition of mGlu4 HD with a NAM (Figure 5).

Asymmetric transduction of mGlu heterodimers

The above data were generated using mGlu2 and mGlu4 subunits carrying a modified C-terminal tail containing a quality control system. We then used another approach to validate our observation not only with mGlu2 and mGlu4 subunits with unmodified C-terminal tails, but also with other possible combinations of mGlu heterodimers (Figure 6). To that aim, we co-expressed two subunits, with one carrying the mutation preventing G protein activation. By specifically activating this mutated subunit, a functional response may only be generated with the heterodimer containing the wild-type subunit, providing the latter can be responsible for G protein activation in the heterodimer.

Using the non-functional mGlu4FS, co-expressed with mGlu2, no signal could be generated upon activation with the mGlu4 agonist L-AP4, in agreement with mGlu4 HD being the G protein-coupling domain in the mGlu2-4 heterodimer (Figure 6A). Consistent with this, activating an mGlu2FS mutant with DCG-IV generated a signal providing this subunit is co-expressed with mGlu4 (Figure 6A). Note that under these experimental conditions, cells expressed three types of dimers, the mGlu2 and mGlu4 homodimers and the mGlu2-4 heterodimer. Accordingly, if mGlu4 was the FS mutated subunit, L-AP4 had no effect, while DCG-IV could generate a signal through mGlu2 homodimers. In contrast, if mGlu2FS mutant was used, DCG-IV could generate a signal through the 2-4 heterodimer, and L-AP4 through the mGlu4 homodimers. Correct expression and function of all constructs was verified (Figure 6-figure supplement 1). These data confirmed that the asymmetric activation of the mGlu2-4 HDs is not the consequence of the presence of the C1-C2 intracellular

domains.

The same approach was conducted with all possible heterodimeric receptors made of mGlu2 or mGlu3 associated with any of the group-III mGluRs: mGlu4, 6, 7 and 8. As depicted in Figure 6C-F and Figure 6-figure supplement 2, similar data were obtained with any of these 4 types of heterodimers for mGlu2 and for mGlu3. These data indicate that in all these cases, the group-III subunit is responsible for G protein activation in these heterodimers. As observed with the mGlu2-4 heterodimer (Figure 4), the mGlu2 NAM, MNI137, inhibited signaling of all these heterodimers (Figure 6C-F). This is consistent with the mGlu2 HD, though not directly involved in G protein coupling, being important to allow the group-III subunit to signal in these heterodimeric receptors.

Discussion

Our data revealed important information on how two G protein-activating units communicate within a heterodimeric complex. We found that in the mGlu2-4 heterodimer, only the mGlu4 subunit activates G proteins, and we revealed a complex allosteric interaction between the two HDs. Indeed, the mGlu2 subunit retains its ability to signal providing its activation is favored using mGlu2 PAMs, or preventing the activation of mGlu4 HD with a NAM. Such findings, schematized in Figure 7, will certainly help elucidate the functional control of one GPCR by another, and how this can be modulated, then providing novel opportunities to decipher the role of possible GPCR heterodimers.

The key information reported here is that, even though both HDs in the mGlu2-4 heterodimer are capable of activating G proteins, only that of mGlu4 does it (Figure 7, State 2). This is not only observed with the mGlu2-4 but with any other heterodimers made of mGlu2 and a group-III mGlu subunits, where the group-III HD is always responsible for coupling. Such asymmetric activation of a GPCR dimer has often been observed (20, 21, 51-54). Even in the mGlu homodimers, only one subunit is active at a time, although in that case, each subunit has the same probability of being active (44-46). For the well-characterized heterodimeric GPCRs, such as the GABA_B and the T1R taste receptors, also one subunit only is responsible for G protein activation (51, 52, 54), although this was assumed to result from the inability of the other subunit to signal. Our data suggest that instead, the inability of signaling of one subunit may result from an inhibitory effect of the other subunit while in its fully active state. This is indeed likely the case for the GABA_B receptor for which the GABA_{B1} subunit, not involved in coupling in the heterodimer, has been reported to signal when expressed alone (55, 56). Similar asymmetric coupling has also been reported for class A GPCR heterodimers, where the activation of one receptor prevents the activation of the other (20, 21, 53). These observations reinforce the idea of a strong negative cooperativity between the HDs in a dimeric GPCR complex, where the activation of one subunit suppresses the ability of the other to signal. This conclusion is further supported by numerous studies reporting negative cooperativity in agonist binding on dimeric GPCRs (13, 57).

While mGlu4 homodimer coupling efficacy measured is lower than that of mGlu2, it is

interesting to note that the coupling efficacy of mGlu2-4 heterodimer is similar to that of mGlu2 receptors. Because in both mGlu4 and mGlu2-4, the G protein activation is mediated by the mGlu4 HD, this means that the mGlu2 subunit potentiates mGlu4 efficacy. Such a low coupling efficacy of mGlu4 homodimers may well be the consequence of a weaker action of the mGlu4 ECD dimer on the HDs, consistent with the weaker coupling of heterodimers containing two mGlu4 ECDs (Figure 2). It may also possibly result in part from another level of interaction between the HDs within a dimeric receptor. Even though the mGlu2 HD does not directly activate the G protein in the heterodimer, it is important for the full activation of the mGlu4 HD (Figure 7). Indeed, the mGlu2 HD likely changes its conformation to exert this positive effect, even though this conformation is not sufficient for G protein coupling (Figure 7). This is well demonstrated by the partial inhibition of the mGlu2-4 activity (mediated by the mGlu4 HD) by a specific mGlu2 NAM known to stabilize the mGlu2 HD in its inactive state (49) (Figure 7, State 3a). Such an action of the mGlu2 HD is even more prominent if the VFT dimer is asymmetrically activated, with only one VFT occupied by an agonist (Figure 7, States 3b, 3c). Such data revealed important allosteric interaction between two HDs in a GPCR dimer, not expected so far. They are however perfectly in line with the role of the GABA_{B1} HD in the activation process of the heterodimeric GABA_B receptor, the latter being involved in a direct activation of the GABA_{B2} HD through an intra-molecular conformational change (58).

Our data then further strengthen the multiple allosteric interactions between class C GPCR domains in the activation process, with the activation of one HD within the dimer being controlled in two ways. The first one is by the reorientation of the VFTs with an efficient coupling when the reorientation is symmetric (both VFTs activated), and a less efficient coupling in case only one VFT is activated (29, 41). Of note, the sequence of the CRDs that link the VFTs to the HDs also plays a role, as indicated here by the differential coupling efficacies of receptor combinations containing either the mGlu2 CRD or the mGlu4 CRD (Figure 2, Figure 2-figure supplement 1, Figure 4D). The second pathway comes from a conformational change in the associated HD likely through a direct interaction between the two HDs in the dimer, consistent with our previous data with the heterodimeric GABA_B

receptor (58). The second component is higher when the first, VFT mediated, is weak, due either to the activation of only one VFT (Figure 4), or to specific combinations of the CRDs (Figure 2, Figure 4D).

Such allosteric interaction most likely results from a contact between the two HDs via an interface that can communicate information from one HD to the other. This can be achieved if the interface involves component of the HD that changes conformation depending on the state of the subunit. Recently, we reported that, even though both HDs in a class C GPCR contact each other through TM4 and 5 in the basal state, as also reported for many class A GPCR dimers (59, 60), we surprisingly identified TM6 as being involved in the dimer interface of the active receptor dimer (38). TM6 is the TM that moves the most during class A GPCR activation (61, 62), also likely in class C GPCRs (23) for which the allosteric coupling between both HDs in a GPCR dimer is of fundamental mechanistic importance. More work is obviously needed to analyze the TM rearrangement in class C GPCR activation.

Another major observation is that it is possible, using small molecules to reorient the G protein coupling from one subunit to the other – i.e. from the mGlu4 HD to the mGlu2 HD in the mGlu2-4 heterodimer (Figure 7, States 4a, 4b). Indeed, by either preventing the activation of the mGlu4 HD with an mGlu4 specific NAM (Figure 7, States 4b), or by stabilizing the mGlu2 HD in its active conformation with a specific mGlu2 PAM (Figure 7, States 4b), the G protein coupling is transferred from the mGlu4 to the mGlu2 subunit. This observation suggests that the mGlu4 HD is likely more prone to reach a G protein activating state than the mGlu2 HD, and the fully active form of mGlu4 HD prevents the mGlu2 HD from reaching a G protein activating state. Such observation opens interesting possibilities to decipher the specific role of each subunit in this mGlu2-4 heterodimer, especially in specific brain area where it is expressed.

There is much interest in the development of allosteric modulators, since these are expected to have less side effects for several reasons (63-66). Such small molecules target a site that is under less pressure during evolution, such that it is possible to identify subtype selective molecules, in contrast to compound acting in the orthosteric binding site highly conserved between homologous receptors. In addition, PAMs do not constantly activate the receptor,

then do not favor receptor desensitization and internalization. Moreover, because they enhance the action of endogenous ligands, they increase the response when and where needed for an improved physiological response. Here we reveal a novel property of such small molecules: their ability to control the asymmetric activation of a GPCR dimer.

Taken together, the present study illustrates the complex allosteric interaction occurring between two associated G protein-activating units, with both positive and negative interactions. Indeed, a conformational change in one subunit is needed for a full G protein activation by its associated subunit, although the interaction also prevents the first subunit from activating G proteins. Because more and more data are consistent with the existence of GPCR heteromers, our finding will certainly bring much interest in elucidating their possible roles in integrating signals targeting either subunit.

Materials and methods

Materials

L-glutamate was purchased from Sigma. DCG-IV, L-AP4, MNI137 and LY487379 were from Tocris Bioscience. LSP4-2022 was provided by Dr. F. Acher (Paris, France). Glutamate-pyruvate transaminase (GPT) was purchased from Roche. Lipofectamine 2000 and Fluo-4-AM were from Life Technologies. SNAP-Green was from NEN Biolabs.

Plasmids and transfection

The pRK5 plasmids encoding the HA-tagged wild-type mGluR2-3-4-6-7-8 from rat were described previously (37). The site-directed mutations in the pRK5 plasmid were generated using QuikChange mutagenesis protocol (Agilent Technologies). The sequence coding C1 (the 47-residue coiled-coil sequence of the C-terminal of GABA_{B1}), or C2 (the 49-residue coiled-coil region of GABA_{B2}), followed by the endoplasmic reticulum retention signal KKTN. ^{HA}mGluR2_{C1KKXX} (2_{C1}) and ^{Flag}mGluR2_{C2KKXX} (2_{C2}) (with and without a N-terminal SNAP tag) have been reported previously (38). Using the same strategy, the last 38 residues in mGluR4 C terminus (HA, flag and SNAP-tagged versions of mGlu4 were used) were replaced by C1KKXX or C2KKXX to obtain ^{HA}mGluR4_{C1KKXX} (4_{C1}), ^{Flag}mGluR4_{C2KKXX} (4_{C2}). The chimeras (2^{VFT}4^{HD}, 4^{VFT}2^{HD}) were obtained by introducing a Bgl II restriction site in both mGlu2 and mGlu4 subunits, Ala497Arg mutation in mGluR2 and same sense mutations at Arg517Ser518 in mGluR4 were induced to make the restriction site. Chimeras (2^{ECD}4^{HD}, 4^{ECD}2^{HD}) were obtained by exchanging the ECD domain before the Pro557 in mGluR2 and Pro577 in mGluR4.

HEK-293 cells (ATCC, CRL-1573, lot: 3449904) were cultured in DMEM supplemented with 10% FBS and transfected by electroporation as described elsewhere. Absence of mycoplasma was routinely checked using the MycoAlert Mycoplasma detection kit (LT07-318 (Lonza, Amboise, France), according to the manufacturer protocol. Ten millions cells were transfected with 2µg of each plasmid of indicated and completed to a total amount of 10µg with the plasmid encoding the pRK5 empty vector. To allow efficient coupling of the receptor to the phospholipase C pathway, cells were also transfected with the

chimeric G protein G α q19 (1 μ g) or G α qo (1 μ g), and the glutamate transporter EAAC1 (1 μ g). For cell-surface expression and functional assays of indicated subunits, experiments were performed after incubation for 36h (12h at 37°C, 5% CO₂ and then 24h at 30°C, 5% CO₂).

SNAP fluorescent-labeled blot experiments

Cells after electroporation, adherent HEK293 cells plated in 12-well plates were labeled with 300 nM SNAP-Green in culture medium at 37 °C for 1 h. Cells were lysed with lysis buffer (50 mM Tris-HCl, pH 7.4, 150 mM NaCl, 1% Nonidet P-40, 0.5% sodium deoxycholate, 0.1% SDS and protease inhibitors) at 4 °C for 1.5 h. After centrifugation at 12,000g for 30 min, supernatants were added with loading buffer (NuPAGE LDSsample buffer 4, Invitrogen) for 10 min. Electrophoresis was performed using precast NuPAGE Novex 8% Tris-acetate gels (Life Technologies) and blotted onto nitrocellulose membranes. Membranes were imaged on an Odyssey infrared scanner (LI-COR Biosciences, Lincoln, NE, USA) at 800 nm for SNAP-Green (38).

Cell surface quantification by ELISA

Cell surface expression of the indicated subunits was detected by ELISA. HA- and Flag-tagged subunits were co-transfected into HEK293 cells seeded into 96-well microplates. Cell surface expression and total expression (treated with 0.05% triton) was detected with a monoclonal rat anti-HA antibody (3F10, Roche) or rat anti-Flag (F1804, Sigma) and a goat anti-rat second antibody coupled to HRP (Jackson ImmunoResearch, West Grove, PA) as previously described (58). Bound antibody was detected by chemoluminescence using SuperSignal substrate (Pierce) and a 2103 EnVision™ Multilabel Plate Reader (Perkin Elmer, Waltham, MA, USA).

Intracellular calcium release and inositol phosphate measurement

Intracellular Ca²⁺ release was measured as described (45). In brief, cells were pre-incubated for 1 h with the Ca²⁺-sensitive Fluo-4 acetoxymethyl ester (Invitrogen). The fluorescence signals (excitation at 485 nm and emission at 525 nm) were then measured for 60 s (Flex-Station, Molecular Devices). Agonist was added after the first 20 s. The Ca²⁺ response is given as the agonist-stimulated fluorescence increase. Concentration response curves were

412 fitted using Graph Pad Prism.

413 Inositol phosphate (IP) accumulation in HEK293 cells co-transfected with indicated subunits
414 was measured after stimulation with agonist for 30 min in 96-well microplates as previously
415 described (45). After incubation in the presence of LiCl (10 mM, 30 min) and termination of
416 the reaction with 0.1 M formic acid, the supernatant was recovered and purified by ion
417 exchange chromatography using DOWEX resin. Radioactivity was measured using a
418 Wallac1450 MicroBeta microplate liquid scintillation counter (Perkin Elmer, Waltham, MA,
419 USA).

420 **Statistical analysis**

421 Statistical analyses were performed on at least three individual data sets analyzed by
422 Graphpad prism using unpaired t-tests.

423

424

Acknowledgements

This work was supported by the National Natural Science Foundation of China (NSFC grant nos. 31420103909, 31711530146, 31511130131, 31100548), the Program of Introducing Talents of Discipline to the Universities of the Ministry of Education (grant no. B08029), Natural Science Foundation of Hubei province (grant no. 2014CFA010) and the Mérieux Research Grants Program of Institut-Mérieux (to J.L.). JPP was supported by the Centre National de la Recherche Scientifique, the Institut National de la Recherche Médicale and by the Fondation pour la Recherche Médicale (grant no. DEQ20130326522), and CisBio bioassays. JG was supported by the Ministerio de Economía y Competitividad (ERA-NET NEURON PCIN-2013-018-C03-02 and SAF2014-58396-R).

Figure Legends

Figure 1. mGlu4 activates G protein in the mGlu2-4 heterodimer.

A) Cartoons illustrating mGlu2 (2-2) and mGlu4 (4-4) homodimers, and mGlu2-4 (2-4 or 4-2) heterodimers with each subunit carrying the quality control C1 or C2 system as C terminal tails, and the indicated HA or Flag tag at their N terminus. B) Quantification of cell surface expressed HA-tagged or Flag-tagged constructs by ELISA on intact cells transfected with the indicated subunits (2_{C1}, 2_{C2}, 4_{C1}, 4_{C2}) alone or together. Data are expressed as means \pm SEM (n \geq 3). **p<0.01, ***p<0.001 (unpaired t test). C, D, E, F) Intracellular Ca²⁺ responses mediated by the indicated subunits upon stimulation with increasing concentrations of glutamate, in the presence of the chimeric Gqi9, with the control subunits (C), the mGlu2 homodimer with no, one or both subunits mutated (D), same with mGlu4 homodimer (E) or mGlu2-4 heterodimer (F). The red cross indicates the subunit carries the FS mutation that prevents G protein activation. Data are expressed as means \pm SEM of triplicates from a typical experiment repeated at least three times.

Figure 2. Asymmetric transduction results from the HDs in the mGlu2-4 heterodimer.

In A), B) and C) cartoons illustrating the heterodimer combinations used with one or both subunits carrying the FS mutation (red cross) that prevents G protein activation are indicated on the top. For each subunit, white domains are from mGlu2, while the grey domains are from mGlu4. The chimeric protein made of mGlu2 ECD and mGlu4 HD is named 2^{ECD}4^{HD} and the reverse chimera named 4^{ECD}2^{HD}. The intracellular Ca²⁺ responses mediated by the indicated subunit compositions (color coded, as indicated on top of the cartoons) upon stimulation with DCG-IV (30 μ M), L-AP4 (30 μ M) or glutamate (1mM) shown at the bottom. A) Data obtained with heterodimers containing both ECDs (VFT and CRD) from mGlu2. B) Data obtained with heterodimers containing both ECDs from mGlu4. C) Data obtained with heterodimers in which the ECDs were swapped between the two subunits. Data are means \pm SEM (n \geq 3). **p<0.01, ***p<0.001 (unpaired t test).

Figure 3. Constitutive activity of disulfide-tethered mGlu2-4 heterodimer is mediated by the mGlu4 subunit.

A) Cartoons illustrating the heterodimer combinations used with mGlu2 or mGlu4 subunits carrying the FS mutation (red cross) that prevents G protein activation (top). The red line linking both CRDs indicates the disulfide bridge that constrains the dimer into an active state. Inositol phosphate (IP) accumulation in cells expressing the dimer combinations after incubation with or without glutamate (1mM). Data are means \pm SEM (n \geq 3). ***p<0.001 (unpaired t test). **B)** On the top, the cartoons indicate the heterodimeric combinations analyzed by western blots (bottom) with or without DTT treatment. The natural inter-subunit disulfide bridge in the control dimer (wt) is indicated in (a), leading to the lack of monomers in the non-reducing conditions. When mutating both Cys involved in this natural crosslink (C121A in mGlu2 and C136A in mGlu4), both subunits can dissociate into monomers even in the absence of DTT (b). Adding a new disulfide bridge in the CRD (L521C in mGlu2 and H523C in mGlu4) (c) restores the subunit cross-linking. By using SNAP-tag labeling with a cell-impermeant fluorescein substrate, only the cell surface subunits are labeled, and then detected on the blot. Data are from a typical experiment repeated three times.

Figure 4. Allosteric regulation of mGlu4-induced signaling by mGlu2 HD.

In each panel, cartoons (color coded) illustrating the dimer compositions used are indicated on the top, and intracellular Ca²⁺ responses mediated by indicated dimer combinations upon stimulation with glutamate (1mM) and increasing concentration of the mGlu2 NAM, MNI137 (purple square). The inactivating FS mutation is shown as a red cross. **A)** Effect of MNI137 on homodimeric mGlu2 and mGlu4 receptors, and on the mGlu2-4 heterodimer carrying or not the FS mutation in the mGlu4 subunit activated by glutamate (blue arrow). **B)** Effect of MNI137 on the constitutively active dimers resulting from the CRD disulfide cross-linking. **C)** Effect of increasing concentrations of MNI137 on the mGlu2-4 heterodimer activated by the mGlu2 agonist DCG-IV (30 μ M, green arrow), L-AP4 (30 μ M, red arrow) or both. **D)** Intracellular Ca²⁺ response under control condition, or after stimulation with DCG-IV (30 μ M, green arrow) with or without MNI137 (10 μ M) with the indicated dimer combinations. Data are means \pm SEM of triplicates from a typical experiment repeated at least three times (A,

B, C), or from three independent experiments (D). ***p<0.001 (unpaired t test).

Figure 5. Switching of the G protein coupling subunit in the mGlu2-4 heterodimer by mGlu2 PAM and mGlu4 NAM.

Intracellular Ca^{2+} response mediated by the indicated subunits upon stimulation with increasing concentration of glutamate with/without a mGlu4 NAM (optoGluNAM4.1, green square, 30 μM) or a mGlu2 PAM (LY487379, yellow triangle, 10 μM). A) The mGlu4 NAM allows mGlu2 HD coupling to G proteins in the heterodimer. B) The mGlu2 PAM allows mGlu2 HD coupling to G proteins. Data are means \pm SEM of triplicates from a typical experiment repeated at least three times.

Figure 6. Asymmetric transduction by mGlu2-groupIII heterodimers.

A-B) schemes illustrating the method used to study the coupling properties of mGlu heterodimers composed of mGlu2 (group-II) and a group-III subunit with the wild-type C-terminal tails. In **A)**, activating specifically the mGlu2 subunit unable to activate G protein (F756S, red cross) can generate a signal only if associated with a functional group-III subunit. **B)** Same as in **A)** with the inactive group-III subunit (F781S, F773S, F784S, F777S in mGlu4-6-7-8, respectively) and a specific group-III agonist. **C-F)** functional coupling of the indicated subunits under the condition indicated on the top (black, control; green, group-II agonist (DCG-IV, 30 μM); blue, group-II agonist with mGlu2 NAM (DCG-IV, 30 μM and MNI137 10 μM); red, group-III agonist (L-AP4, 30 μM for mGlu4-6-8, LSP4-2022, 300 μM for mGlu7). **C)** Data obtained with cells expressing both mGlu2 and mGlu4, with either the inactive mGlu2 (2^{X}) or the inactive mGlu4 (4^{X}). **D, E and F)**, same as in **C** using mGlu6, mGlu7 or mGlu8 constructs, respectively. Data are means \pm SEM ($n \geq 3$). **p<0.01, ***p<0.001 (unpaired t test).

Figure 7. Scheme illustrating the activation mechanism and allosteric control of mGlu2-4 heterodimer. State 1: the inactive heterodimer in its basal state. **State 2:** Glutamate (blue disk) activation of both subunits leads to G protein activation by mGlu4 HD, also involving a conformational change in the mGlu2 HD. **State 3:** the addition of mGlu2 NAM

528 (purple square) largely decreases coupling efficacy of the mGlu2-4 heterodimer activated by
529 glutamate (**3a**), or suppress detectable coupling if either the mGlu2 (**3b**) or mGlu4 (**3c**) is
530 specifically activated. **State 4**: heterodimeric mGlu2-4 coupling through the mGlu2 HD
531 thanks to the addition of a mGlu4 NAM (green square, **4a**), or a mGlu2 PAM (yellow triangle,
532 **4b**).

533

Legends to Figure supplements

Figure 1 – figure supplement 1. G protein coupling of the mGlu subunits with C1 or C2 tail.

Intracellular Ca^{2+} response mediated by indicated subunits co-expressed with the chimeric Gqi9 upon stimulation with DCG-IV ($30\ \mu\text{M}$, green), L-AP4 ($30\ \mu\text{M}$, red) or glutamate (1mM , blue). Data are means \pm SEM of triplicates from a typical experiment repeated at least three times.

Figure 1 – figure supplement 2. Cell surface and total expression of various mGlu dimer combination

Quantification of cell surface-total expression of HA-tagged or Flag-tagged constructs (as indicated in Fig 1) by ELISA on intact cells transfected with indicated subunits. Data were obtained from a same cells used for with Fig 1D, E, F and expressed as means \pm SEM of triplicates from a typical experiment repeated at least three times.

Figure 1 – figure supplement 3. mGlu4 is responsible for G protein coupling in the mGlu2-4 heterodimer.

(A) Intracellular Ca^{2+} responses mediated by indicated subunits upon stimulation with increasing concentration of glutamate, in the presence of the chimeric Gqi9. B) Cartoons illustrating the receptor combinations used in panels C and D. C) Intracellular Ca^{2+} response mediated by indicated subunits co-expressed with Gqi9 upon stimulation with DCG-IV ($30\ \mu\text{M}$), L-AP4 ($30\ \mu\text{M}$), or DCG-IV + L-AP4. D) Same as in C with Gqo. Data are means \pm SEM of triplicates from a typical experiment repeated at least three times.

Figure 2 – figure supplement 1. Asymmetric transduction results from the HDs in the mGlu2-4 heterodimer.

Same as Fig 2 excepted that only the VFT is swapped, and not the entire CRD. In A), B) and C) cartoons illustrating the heterodimer combinations used with one or both subunits carrying the FS mutation (red cross) that prevents G protein activation are indicated on the top. For each subunit, white domains are from mGlu2, while the grey domains are from mGlu4. The chimeric protein made of mGlu2 VFT and mGlu4 CRD+HD is named 2^{VFT}4^{HD} and the reverse chimera named 4^{VFT}2^{HD}. The intracellular Ca²⁺ responses mediated by the indicated subunit compositions (color coded, as indicated on top of the cartoons) upon stimulation with DCG-IV (30 μ M), L-AP4 (30 μ M) or glutamate (1mM) shown at the bottom. A) Data obtained with heterodimers containing both VFT from mGlu2. B) Data obtained with heterodimers containing both VFTs from mGlu4. C) Data obtained with heterodimers in which the VFTs were swapped between the two subunits. Data are means \pm SEM (n \geq 3). **p<0.01, ***p<0.001 (unpaired t test).

Figure 2 – figure supplement 2. Cell surface and total expression of various mGlu dimer combination

Quantification of cell surface-total expression of HA-tagged or Flag-tagged constructs by ELISA on intact cells transfected with the indicated subunits as in Fig. 2. Data were generated from the same cells used in Fig 2 and are means \pm SEM of triplicates from a typical experiment repeated at least three times.

Figure 2 – figure supplement 3. Cell surface and total expression of various mGlu dimer combination

Quantification of cell surface-total expression of HA-tagged or Flag-tagged constructs by ELISA on intact cells transfected with the indicated subunits as in Sup Fig. 4. Data were generated from the same cells used in Sup Fig 4 and are means \pm SEM of triplicates from a typical experiment repeated at least three times.

Figure 3 – figure supplement 1. Cell surface and total expression of various mGlu dimer combination

Quantification of cell surface-total expression of HA-tagged or Flag-tagged constructs by ELISA on intact cells transfected with the indicated subunits as in Fig. 3A. Data were generated from the same cells used in Fig 3A and are means \pm SEM of triplicates from a typical experiment repeated at least three times.

Figure 6 – figure supplement 1. Expression and function of the indicated subunits. (A) Quantification of cell expression of HA-tagged constructs by ELISA on cells transfected with the indicated subunits. (B) Intracellular Ca^{2+} response mediated by the indicated subunits upon stimulation with DCG-IV (30 μM) for mGluR2-3, L-AP4 (30 μM) for mGluR4-6-8, LSP4-2022 (300 μM) for mGluR7 or glutamate (1mM). Data in A and B were generated from the same transfected cells, and are means \pm SEM of triplicates from a typical experiment repeated at least three times.

Figure 6 – figure supplement 2. Asymmetric transduction by mGlu2-groupIII heterodimers.

Same as Fig 7, except mGlu3 was used instead of mGlu2. A) and B) schemes illustrating the method used to study the coupling properties of mGlu heterodimers composed of mGlu3 (group-II) and a group-III subunit. In A), activating specifically the mGlu3 subunit unables to activate G protein (F765S, red cross) can generate a signal only if associated with a functional group-III subunit. B) Same as in A) with the inactive group-III subunit (F781S, F773S, F784S, F777S in mGlu4-6-7-8, respectively) and a specific group-III agonist. C-D) functional coupling of the indicated subunits under the condition indicated on the top (black, control; green, group-II agonist (DCG-IV, 30 μM); blue, group-II agonist with mGlu2/3 NAM (DCG-IV, 30 μM and MNI137 10 μM); red, group-III agonist (L-AP4, 30 μM for mGlu4-6-8, LSP4-2022, 300 μM for mGlu7). C) Data obtained with cells expressing both mGlu3 and mGlu4, with either the inactive mGlu3 (3^X) or the inactive mGlu4 (4^X). D, E and

619 F) same as in C using mGlu6, mGlu7 or mGlu8 constructs, respectively. Data are means \pm
620 SEM (n \geq 3). **p<0.01, ***p<0.001 (unpaired t test).

621

622

623

Legends to Source data files

Figure 1-source data file 1: Glutamate potency at the indicated heterodimers

Intracellular Ca^{2+} responses mediated by the indicated subunits upon stimulation with increasing concentrations of glutamate. 2^x and 4^x indicated subunits carrying the F756S (mGlu2) or F781S (mGlu4) mutation preventing G protein activation. Data represent the means \pm SEM of (n) independent experiments. N.D., not determined.

Figure 4-source data file 1: MNI137 potency at the indicated mGlu dimers.

Intracellular Ca^{2+} response mediated by indicated subunits upon stimulation with glutamate (1mM) and inhibited by increasing concentration of MNI137. Data represent the means \pm SEM of (n) independent experiments. N.D., not determined.

Figure 4-source data file 2: MNI137 potency at the indicated mGlu dimers.

Inositol phosphate (IP) accumulation in cells expressed indicated subunits, which have constitutive activation, upon inhibition with increasing concentration of MNI137. Data represent the means \pm SEM of (n) independent experiments. N.D., not determined.

Figure 4-source data file 3: MNI137 potency at the indicated heterodimers

Intracellular Ca^{2+} response mediated by indicated heterodimer upon stimulation with DCG-IV (30 μ M), L-AP4 (30 μ M) or DCG-IV (30 μ M) + L-AP4 (30 μ M) and inhibited by increasing concentration of MNI137. Data represent the means \pm SEM of (n) independent experiments. N.D., not determined.

Figure 5-source data file 1: Glutamate potency at the indicated heterodimers and in the presence or absence of the indicated allosteric modulators.

Intracellular Ca^{2+} response mediated by indicated subunits upon stimulation with increasing concentration of glutamate with/without optoGluNAM4.1 (30 μ M) or LY487379 (10 μ M). Data represent the means \pm SEM of (n) independent experiments. N.D., not determined.

654 **References**

- 655 1. M. Klingenberg, Membrane protein oligomeric structure and transport function. *Nature* **290**,
656 449-454 (1981).
- 657 2. M. W. Salter, D1 and NMDA receptors hook up: expanding on an emerging theme. *Trends*
658 *Neurosci* **26**, 235-237 (2003).
- 659 3. C. Altier, H. Khosravani, R. M. Evans, S. Hameed, J. B. Peloquin, B. A. Vartian, L. Chen, A. M.
660 Beedle, S. S. Ferguson, A. Mezghrani, S. J. Dubel, E. Bourinet, J. E. McRory, G. W. Zamponi,
661 ORL1 receptor-mediated internalization of N-type calcium channels. *Nat Neurosci* **9**, 31-40
662 (2006).
- 663 4. J. Gonzalez-Maeso, R. L. Ang, T. Yuen, P. Chan, N. V. Weisstaub, J. F. Lopez-Gimenez, M. Zhou,
664 Y. Okawa, L. F. Callado, G. Milligan, J. A. Gingrich, M. Filizola, J. J. Meana, S. C. Sealton,
665 Identification of a serotonin/glutamate receptor complex implicated in psychosis. *Nature* **452**,
666 93-97 (2008).
- 667 5. M. C. Lagerstrom, H. B. Schioth, Structural diversity of G protein-coupled receptors and
668 significance for drug discovery. *Nat Rev Drug Discov* **7**, 339-357 (2008).
- 669 6. D. El Moustaine, S. Granier, E. Doumazane, P. Scholler, R. Rahmeh, P. Bron, B. Mouillac, J. L.
670 Baneres, P. Rondard, J. P. Pin, Distinct roles of metabotropic glutamate receptor dimerization
671 in agonist activation and G-protein coupling. *Proc Natl Acad Sci U S A* **109**, 16342-16347
672 (2012).
- 673 7. J. F. White, J. Grodnitzky, J. M. Louis, L. B. Trinh, J. Shiloach, J. Gutierrez, J. K. Northup, R.
674 Grisshammer, Dimerization of the class A G protein-coupled neurotensin receptor NTS1 alters
675 G protein interaction. *Proc Natl Acad Sci U S A* **104**, 12199-12204 (2007).
- 676 8. M. R. Whorton, M. P. Bokoch, S. G. Rasmussen, B. Huang, R. N. Zare, B. Kobilka, R. K.
677 Sunahara, A monomeric G protein-coupled receptor isolated in a high-density lipoprotein
678 particle efficiently activates its G protein. *Proc Natl Acad Sci U S A* **104**, 7682-7687 (2007).
- 679 9. L. Prezeau, M. L. Rives, L. Comps-Agrar, D. Maurel, J. Kniazeff, J. P. Pin, Functional crosstalk
680 between GPCRs: with or without oligomerization. *Curr Opin Pharmacol* **10**, 6-13 (2010).
- 681 10. S. Ferre, V. Casado, L. A. Devi, M. Filizola, R. Jockers, M. J. Lohse, G. Milligan, J. P. Pin, X.
682 Guitart, G protein-coupled receptor oligomerization revisited: functional and pharmacological
683 perspectives. *Pharmacological reviews* **66**, 413-434 (2014).
- 684 11. I. Gomes, M. A. Ayoub, W. Fujita, W. C. Jaeger, K. D. Pflieger, L. A. Devi, G Protein-Coupled
685 Receptor Heteromers. *Annu Rev Pharmacol Toxicol* **56**, 403-425 (2016).
- 686 12. D. Maurel, L. Comps-Agrar, C. Brock, M.-L. Rives, E. Bourrier, M. A. Ayoub, H. Bazin, N. Tinel, T.
687 Durroux, L. Prézeau, E. Trinquet, J.-P. Pin, Cell surface protein-protein interaction analysis with
688 combined time-resolved FRET and snap-tag technologies: application to GPCR
689 oligomerization. *Nat Methods* **5**, 561-567 (2008).
- 690 13. L. Albizu, M. Cottet, M. Kralikova, S. Stoev, R. Seyer, I. Brabet, T. Roux, H. Bazin, E. Bourrier, L.
691 Lamarque, C. Breton, M.-L. Rives, A. Newman, J. Javitch, E. Trinquet, M. Manning, J.-P. Pin, B.
692 Mouillac, T. Durroux, Time-resolved FRET between GPCR ligands reveals oligomers in native
693 tissues. *Nature Chemical Biology* **6**, 587-594 (2010).
- 694 14. M. Bellot, S. Galandrin, C. Boularan, H. J. Matthies, F. Despas, C. Denis, J. Javitch, S. Mazeres, S.
695 J. Sanni, V. Pons, M. H. Seguelas, J. L. Hansen, A. Pathak, A. Galli, J. M. Senard, C. Gales, Dual

agonist occupancy of AT1-R-alpha2C-AR heterodimers results in atypical Gs-PKA signaling. *Nat Chem Biol* **11**, 271-279 (2015).

15. J. Wertman, D. J. Dupre, G protein-coupled receptor dimers: look like their parents, but act like teenagers! *J Recept Signal Transduct Res* **33**, 135-138 (2013).

16. M. Fribourg, J. L. Moreno, T. Holloway, D. Provasi, L. Baki, R. Mahajan, G. Park, S. K. Adney, C. Hatcher, J. M. Eltit, J. D. Ruta, L. Albizu, Z. Li, A. Umali, J. Shim, A. Fabiato, A. D. MacKerell, Jr., V. Brezina, S. C. Sealton, M. Filizola, J. Gonzalez-Maeso, D. E. Logothetis, Decoding the signaling of a GPCR heteromeric complex reveals a unifying mechanism of action of antipsychotic drugs. *Cell* **147**, 1011-1023 (2011).

17. E. Urizar, H. Yano, R. Kolster, C. Gales, N. Lambert, J. A. Javitch, CODA-RET reveals functional selectivity as a result of GPCR heteromerization. *Nat Chem Biol* **7**, 624-630 (2011).

18. M. Bouvier, T. E. Hebert, CrossTalk proposal: Weighing the evidence for Class A GPCR dimers, the evidence favours dimers. *J Physiol* **592**, 2439-2441 (2014).

19. N. A. Lambert, J. A. Javitch, CrossTalk opposing view: Weighing the evidence for class A GPCR dimers, the jury is still out. *J Physiol* **592**, 2443-2445 (2014).

20. J. P. Vilardaga, V. O. Nikolaev, K. Lorenz, S. Ferrandon, Z. Zhuang, M. J. Lohse, Conformational cross-talk between alpha2A-adrenergic and mu-opioid receptors controls cell signaling. *Nat Chem Biol* **4**, 126-131 (2008).

21. Y. Han, I. S. Moreira, E. Urizar, H. Weinstein, J. A. Javitch, Allosteric communication between protomers of dopamine class A GPCR dimers modulates activation. *Nat Chem Biol* **5**, 688-695 (2009).

22. J. Kniazeff, L. Prezeau, P. Rondard, J. P. Pin, C. Goudet, Dimers and beyond: The functional puzzles of class C GPCRs. *Pharmacol Ther* **130**, 9-25 (2011).

23. J.-P. Pin, B. Bettler, Organisation and functions of macromolecular mGlu and GABAB receptor complexes. *Nature* **540**, 60-68 (2016).

24. E. Doumazane, P. Scholler, J. M. Zwier, E. Trinquet, P. Rondard, J. P. Pin, A new approach to analyze cell surface protein complexes reveals specific heterodimeric metabotropic glutamate receptors. *FASEB J* **25**, 66-77 (2011).

25. P. J. Kammermeier, Functional and pharmacological characteristics of metabotropic glutamate receptors 2/4 heterodimers. *Mol Pharmacol* **82**, 438-447 (2012).

26. N. J. Pandya, R. V. Klaassen, R. C. van der Schors, J. A. Slotman, A. Houtsmuller, A. B. Smit, K. W. Li, Group 1 metabotropic glutamate receptors 1 and 5 form a protein complex in mouse hippocampus and cortex. *Proteomics* **16**, 2698-2705 (2016).

27. S. Yin, M. J. Noetzel, K. A. Johnson, R. Zamorano, N. Jalan-Sakrikar, K. J. Gregory, P. J. Conn, C. M. Niswender, Selective actions of novel allosteric modulators reveal functional heteromers of metabotropic glutamate receptors in the CNS. *J Neurosci* **34**, 79-94 (2014).

28. F. Ferraguti, T. Klausberger, P. Cobden, A. Baude, J. D. Roberts, P. Szucs, A. Kinoshita, R. Shigemoto, P. Somogyi, Y. Dalezios, Metabotropic glutamate receptor 8-expressing nerve terminals target subsets of GABAergic neurons in the hippocampus. *J Neurosci* **25**, 10520-10536 (2005).

29. D. Moreno Delgado, T. C. Moller, J. Ster, J. Giraldo, D. Maurel, X. Rovira, P. Scholler, J. M. Zwier, J. Perroy, T. Durroux, E. Trinquet, L. Prezeau, P. Rondard, J. P. Pin, Pharmacological evidence for a metabotropic glutamate receptor heterodimer in neuronal cells. *Elife* **6**, (2017).

30. C. M. Niswender, C. K. Jones, X. Lin, M. Bubser, A. Thompson Gray, A. L. Blobaum, D. W.

Engers, A. L. Rodriguez, M. T. Loch, J. S. Daniels, C. W. Lindsley, C. R. Hopkins, J. A. Javitch, P. J. Conn, Development and Antiparkinsonian Activity of VU0418506, a Selective Positive Allosteric Modulator of Metabotropic Glutamate Receptor 4 Homomers without Activity at mGlu2/4 Heteromers. *ACS Chem Neurosci* **7**, 1201-1211 (2016).

31. H. Wu, C. Wang, K. J. Gregory, G. W. Han, H. P. Cho, Y. Xia, C. M. Niswender, V. Katritch, J. Meiler, V. Cherezov, P. J. Conn, R. C. Stevens, Structure of a class C GPCR metabotropic glutamate receptor 1 bound to an allosteric modulator. *Science* **344**, 58-64 (2014).

32. A. S. Dore, K. Okrasa, J. C. Patel, M. Serrano-Vega, K. Bennett, R. M. Cooke, J. C. Errey, A. Jazayeri, S. Khan, B. Tehan, M. Weir, G. R. Wiggan, F. H. Marshall, Structure of class C GPCR metabotropic glutamate receptor 5 transmembrane domain. *Nature* **511**, 557-562 (2014).

33. N. Kunishima, Y. Shimada, Y. Tsuji, T. Sato, M. Yamamoto, T. Kumasaka, S. Nakanishi, H. Jingami, K. Morikawa, Structural basis of glutamate recognition by a dimeric metabotropic glutamate receptor. *Nature* **407**, 971-977 (2000).

34. D. Tsuchiya, N. Kunishima, N. Kamiya, H. Jingami, K. Morikawa, Structural views of the ligand-binding cores of a metabotropic glutamate receptor complexed with an antagonist and both glutamate and Gd3+. *Proc Natl Acad Sci U S A* **99**, 2660-2665 (2002).

35. E. Doumazane, P. Scholler, L. Fabre, J. M. Zwier, E. Trinquet, J. P. Pin, P. Rondard, Illuminating the activation mechanisms and allosteric properties of metabotropic glutamate receptors. *Proc Natl Acad Sci U S A* **110**, E1416-1425 (2013).

36. P. Rondard, J. Liu, S. Huang, F. Malhaire, C. Vol, A. Pinault, G. Labesse, J. P. Pin, Coupling of agonist binding to effector domain activation in metabotropic glutamate-like receptors. *J Biol Chem* **281**, 24653-24661 (2006).

37. S. Huang, J. Cao, M. Jiang, G. Labesse, J. Liu, J. P. Pin, P. Rondard, Interdomain movements in metabotropic glutamate receptor activation. *Proc Natl Acad Sci U S A* **108**, 15480-15485 (2011).

38. L. Xue, X. Rovira, P. Scholler, H. Zhao, J. Liu, J. P. Pin, P. Rondard, Major ligand-induced rearrangement of the heptahelical domain interface in a GPCR dimer. *Nat Chem Biol* **11**, 134-140 (2015).

39. L. Olofsson, S. Felekyan, E. Doumazane, P. Scholler, L. Fabre, J. M. Zwier, P. Rondard, C. A. Seidel, J. P. Pin, E. Margeat, Fine tuning of sub-millisecond conformational dynamics controls metabotropic glutamate receptors agonist efficacy. *Nat Commun* **5**, 5206 (2014).

40. R. Vafabakhsh, J. Levitz, E. Y. Isacoff, Conformational dynamics of a class C G-protein-coupled receptor. *Nature* **524**, 497-501 (2015).

41. J. Kniazeff, A. S. Bessis, D. Maurel, H. Ansanay, L. Prezeau, J. P. Pin, Closed state of both binding domains of homodimeric mGlu receptors is required for full activity. *Nat Struct Mol Biol* **11**, 706-713 (2004).

42. C. Brock, N. Oueslati, S. Soler, L. Boudier, P. Rondard, J. P. Pin, Activation of a dimeric metabotropic glutamate receptor by intersubunit rearrangement. *J Biol Chem* **282**, 33000-33008 (2007).

43. J. Levitz, C. Habrian, S. Bharill, Z. Fu, R. Vafabakhsh, E. Y. Isacoff, Mechanism of Assembly and Cooperativity of Homomeric and Heteromeric Metabotropic Glutamate Receptors. *Neuron* **92**, 143-159 (2016).

44. V. Hlavackova, U. Zabel, D. Frankova, J. Batz, C. Hoffmann, L. Prezeau, J. P. Pin*, J. Blahos*, M. J. Lohse*, Sequential inter- and intrasubunit rearrangements during activation of dimeric

metabotropic glutamate receptor 1. *Science signaling* **5**, ra59 (2012).

45. V. Hlavackova, C. Goudet, J. Kniazeff, A. Zikova, D. Maurel, C. Vol, J. Trojanova, L. Prezeau, J. P. Pin, J. Blahos, Evidence for a single heptahelical domain being turned on upon activation of a dimeric GPCR. *EMBO J* **24**, 499-509 (2005).

46. C. Goudet, J. Kniazeff, V. Hlavackova, F. Malhaire, D. Maurel, F. Acher, J. Blahos, L. Prezeau, J. P. Pin, Asymmetric functioning of dimeric metabotropic glutamate receptors disclosed by positive allosteric modulators. *J Biol Chem* **280**, 24380-24385 (2005).

47. B. R. Conklin, Z. Farfel, K. D. Lustig, D. Julius, H. R. Bourne, Substitution of three amino acids switches receptor specificity of Gq alpha to that of Gi alpha. *Nature* **363**, 274-276 (1993).

48. J. Blahos II, S. Mary, J. Perroy, C. De Colle, I. Brabet, J. Bockaert, J.-P. Pin, Extreme C-terminus of G-protein α -subunits contains a site that discriminates between Gi-coupled metabotropic glutamate receptors. *J. Biol. Chem.* **273**, 25765-25769 (1998).

49. K. Hemstapat, H. Da Costa, Y. Nong, A. E. Brady, Q. Luo, C. M. Niswender, G. D. Tamagnan, P. J. Conn, A novel family of potent negative allosteric modulators of group II metabotropic glutamate receptors. *J Pharmacol Exp Ther* **322**, 254-264 (2007).

50. X. Rovira, A. Trapero, S. Pittolo, C. Zussy, A. Faucherre, C. Jopling, J. Giraldo, J. P. Pin, P. Gorostiza, C. Goudet, A. Llebaria, OptoGluNAM4.1, a Photoswitchable Allosteric Antagonist for Real-Time Control of mGlu4 Receptor Activity. *Cell Chem Biol* **23**, 929-934 (2016).

51. T. Galvez, B. Duthey, J. Kniazeff, J. Blahos, G. Rovelli, B. Bettler, L. Prézeau, J.-P. Pin, Allosteric interactions between GB1 and GB2 subunits are required for optimal GABAB receptor function. *EMBO J.* **20**, 2152-2159 (2001).

52. B. Duthey, S. Caudron, J. Perroy, B. Bettler, L. Fagni, J.-P. Pin, L. Prézeau, A single subunit (GB2) is required for G-protein activation by the heterodimeric GABAB receptor. *J. Biol. Chem.* **277**, 3236-3241 (2002).

53. A. Levoe, J. Dam, M. A. Ayoub, J. L. Guillaume, C. Couturier, P. Delagrange, R. Jockers, The orphan GPR50 receptor specifically inhibits MT1 melatonin receptor function through heterodimerization. *EMBO J* **25**, 3012-3023 (2006).

54. H. Xu, L. Staszewski, H. Tang, E. Adler, M. Zoller, X. Li, Different functional roles of T1R subunits in the heteromeric taste receptors. *Proc Natl Acad Sci U S A* **101**, 14258-14263 (2004).

55. G. A. Baloucoun, L. Chun, W. Zhang, C. Xu, S. Huang, Q. Sun, Y. Wang, H. Tu, J. Liu, GABAB receptor subunit GB1 at the cell surface independently activates ERK1/2 through IGF-1R transactivation. *PLoS One* **7**, e39698 (2012).

56. M. Richer, M. David, L. R. Villeneuve, P. Trieu, N. Ethier, D. Petrin, A. M. Mamarbachi, T. E. Hebert, GABA-B(1) receptors are coupled to the ERK1/2 MAP kinase pathway in the absence of GABA-B(2) subunits. *J Mol Neurosci* **38**, 67-79 (2009).

57. E. Urizar, L. Montanelli, T. Loy, M. Bonomi, S. Swillens, C. Gales, M. Bouvier, G. Smits, G. Vassart, S. Costagliola, Glycoprotein hormone receptors: link between receptor homodimerization and negative cooperativity. *EMBO J* **24**, 1954-1964 (2005).

58. C. Monnier, H. Tu, E. Bourrier, C. Vol, L. Lamarque, E. Trinquet, J.-P. Pin*, P. Rondard, Transactivation between 7TM domains: implication in heterodimeric GABAB receptor activation *EMBO J* **30**, 32-42 (2011).

59. W. Guo, L. Shi, M. Filizola, H. Weinstein, J. A. Javitch, Crosstalk in G protein-coupled receptors: changes at the transmembrane homodimer interface determine activation. *Proc Natl Acad Sci*

828 *U S A* **102**, 17495-17500 (2005).

829 60. A. Manglik, A. C. Kruse, T. S. Kobilka, F. S. Thian, J. M. Mathiesen, R. K. Sunahara, L. Pardo, W. I.

830 Weis, B. K. Kobilka, S. Granier, Crystal structure of the micro-opioid receptor bound to a

831 morphinan antagonist. *Nature* **485**, 321-326 (2012).

832 61. S. G. Rasmussen, H. J. Choi, J. J. Fung, E. Pardon, P. Casarosa, P. S. Chae, B. T. Devree, D. M.

833 Rosenbaum, F. S. Thian, T. S. Kobilka, A. Schnapp, I. Konetzki, R. K. Sunahara, S. H. Gellman, A.

834 Pautsch, J. Steyaert, W. I. Weis, B. K. Kobilka, Structure of a nanobody-stabilized active state

835 of the beta(2) adrenoceptor. *Nature* **469**, 175-180 (2011).

836 62. S. G. Rasmussen, B. T. DeVree, Y. Zou, A. C. Kruse, K. Y. Chung, T. S. Kobilka, F. S. Thian, P. S.

837 Chae, E. Pardon, D. Calinski, J. M. Mathiesen, S. T. Shah, J. A. Lyons, M. Caffrey, S. H. Gellman,

838 J. Steyaert, G. Skiniotis, W. I. Weis, R. K. Sunahara, B. K. Kobilka, Crystal structure of the beta2

839 adrenergic receptor-Gs protein complex. *Nature* **477**, 549-555 (2011).

840 63. J. P. Changeux, A. Christopoulos, Allosteric Modulation as a Unifying Mechanism for Receptor

841 Function and Regulation. *Cell* **166**, 1084-1102 (2016).

842 64. P. J. Conn, C. W. Lindsley, J. Meiler, C. M. Niswender, Opportunities and challenges in the

843 discovery of allosteric modulators of GPCRs for treating CNS disorders. *Nat Rev Drug Discov*

844 **13**, 692-708 (2014).

845 65. D. J. Foster, P. J. Conn, Allosteric Modulation of GPCRs: New Insights and Potential Utility for

846 Treatment of Schizophrenia and Other CNS Disorders. *Neuron* **94**, 431-446 (2017).

847 66. L. T. May, K. Leach, P. M. Sexton, A. Christopoulos, Allosteric modulation of G protein-coupled

848 receptors. *Annu Rev Pharmacol Toxicol* **47**, 1-51 (2007).

849

Figure 1

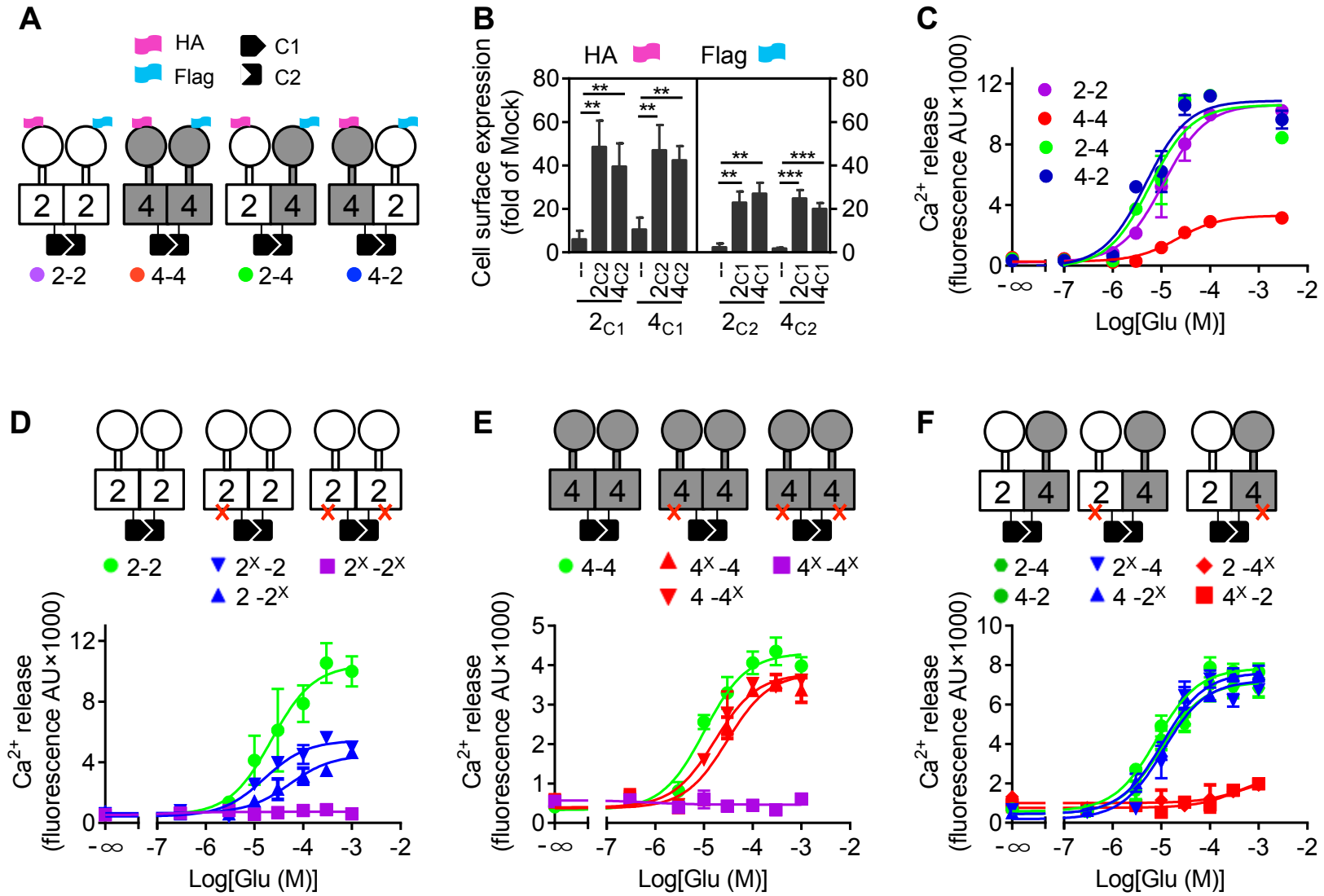


Figure 2

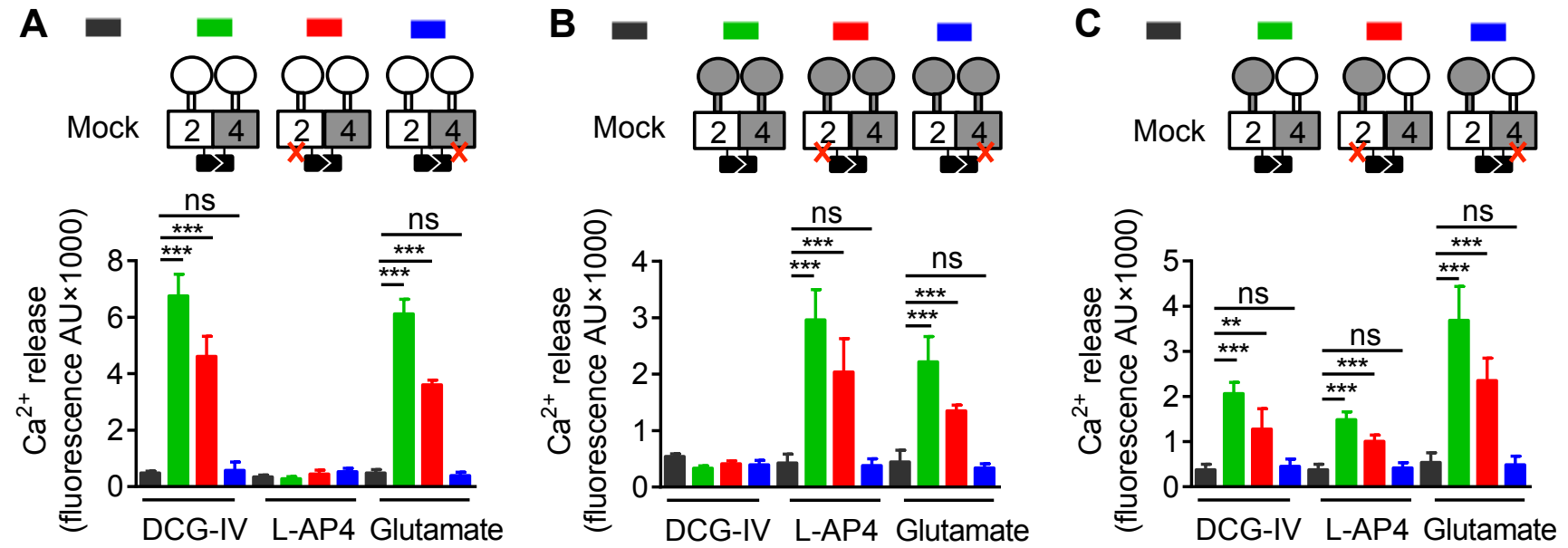


Figure 3

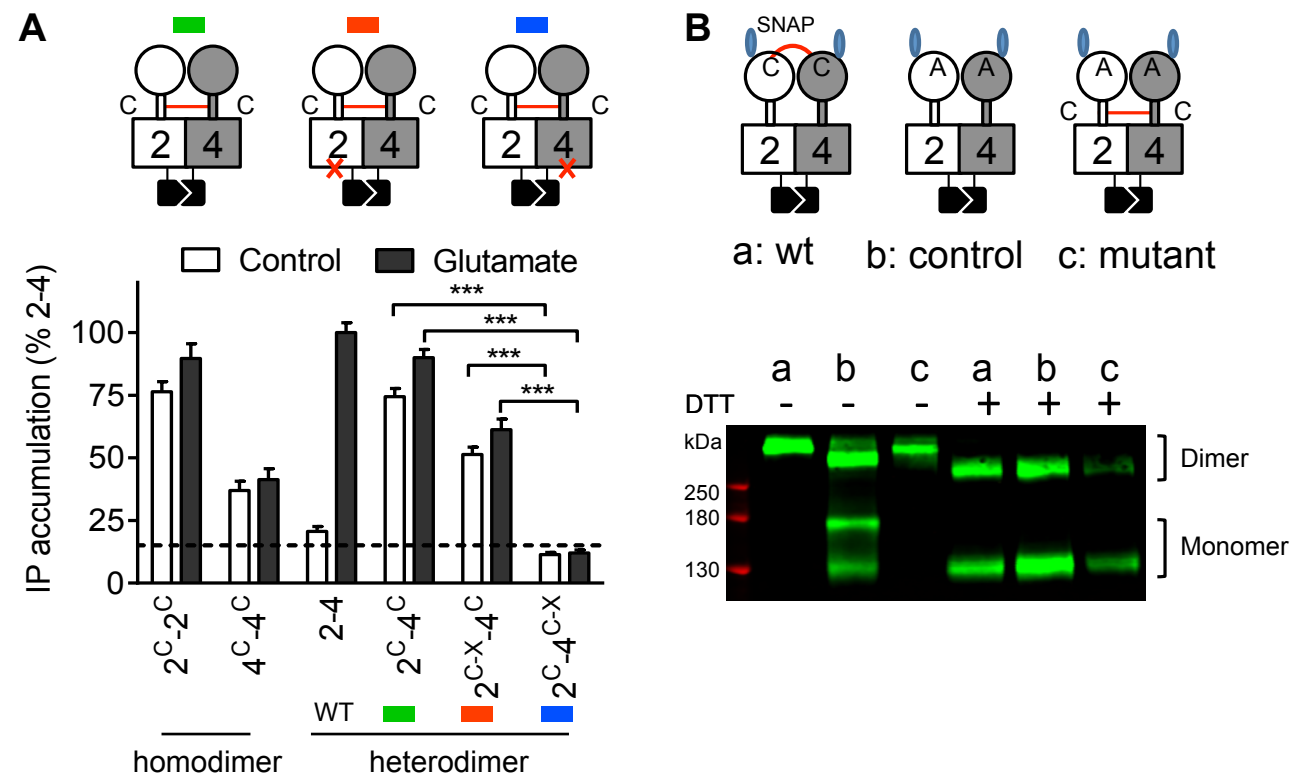


Figure 4

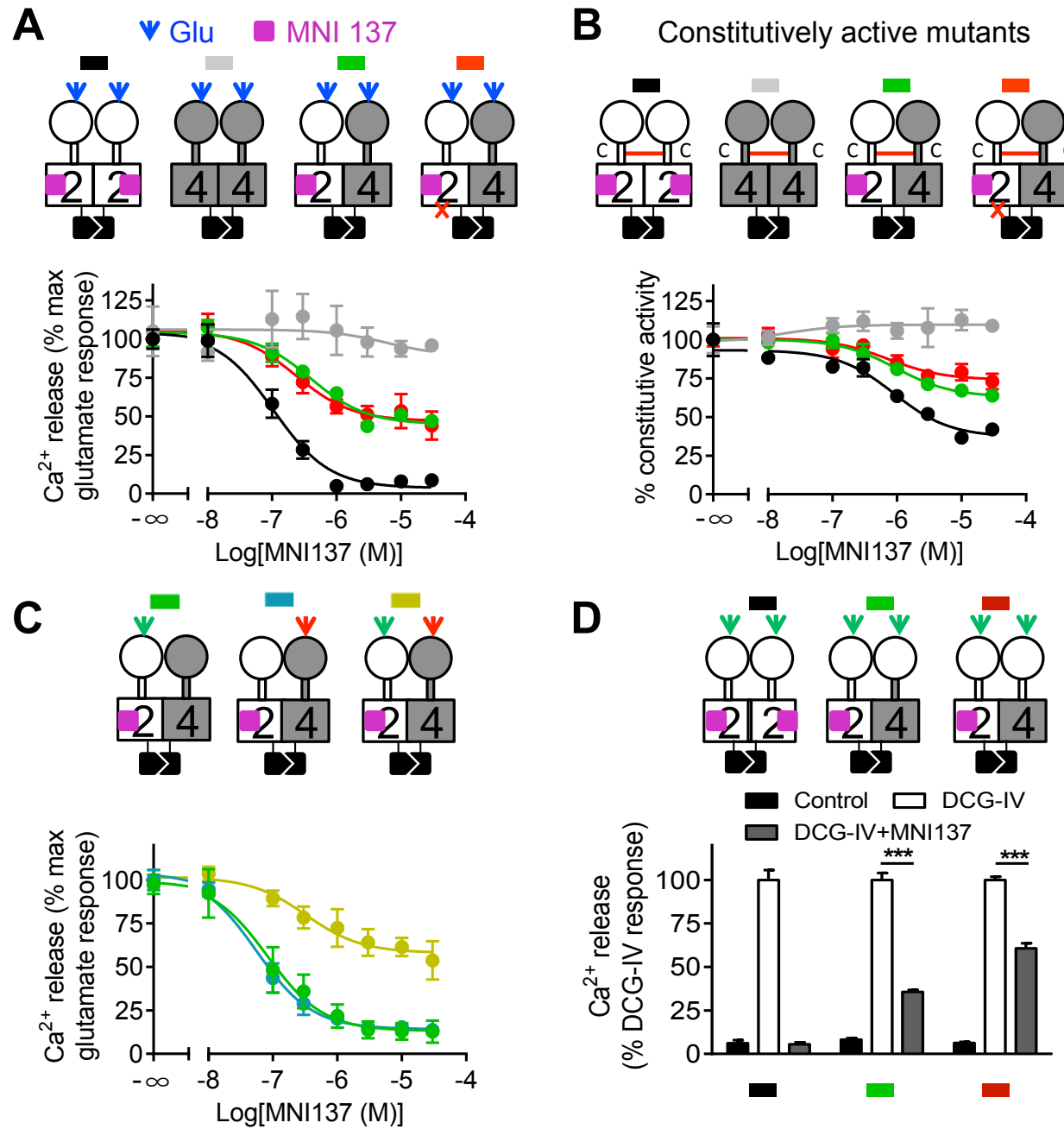


Figure 5

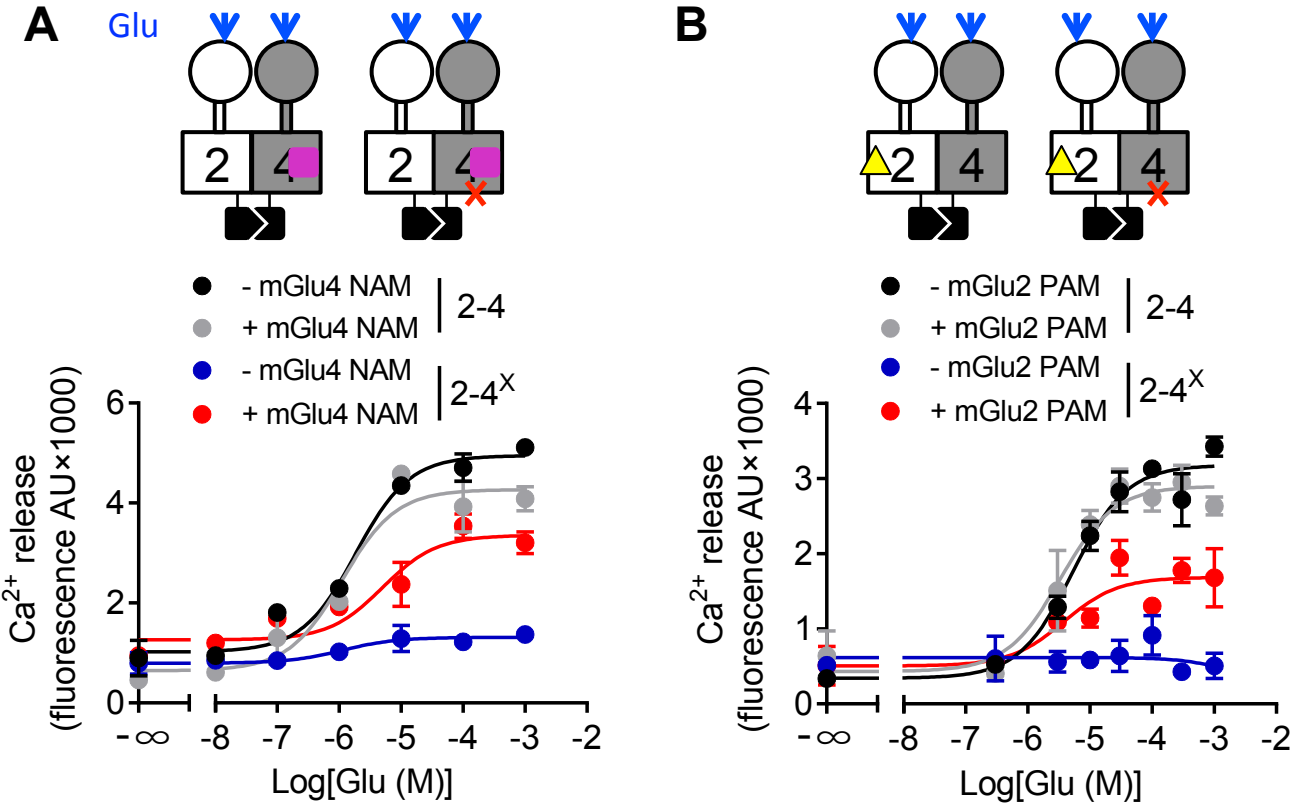


Figure 6

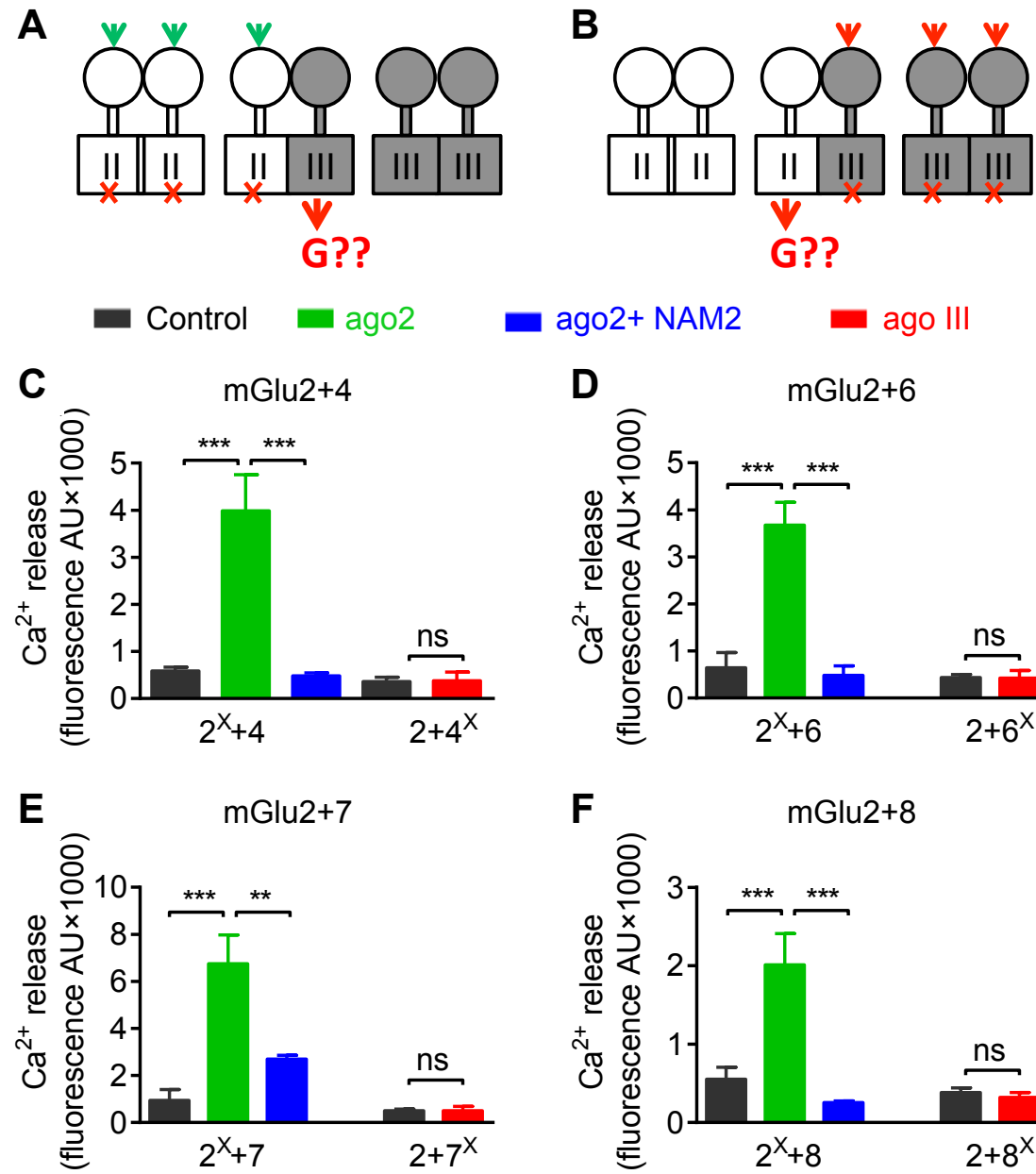


Figure 7

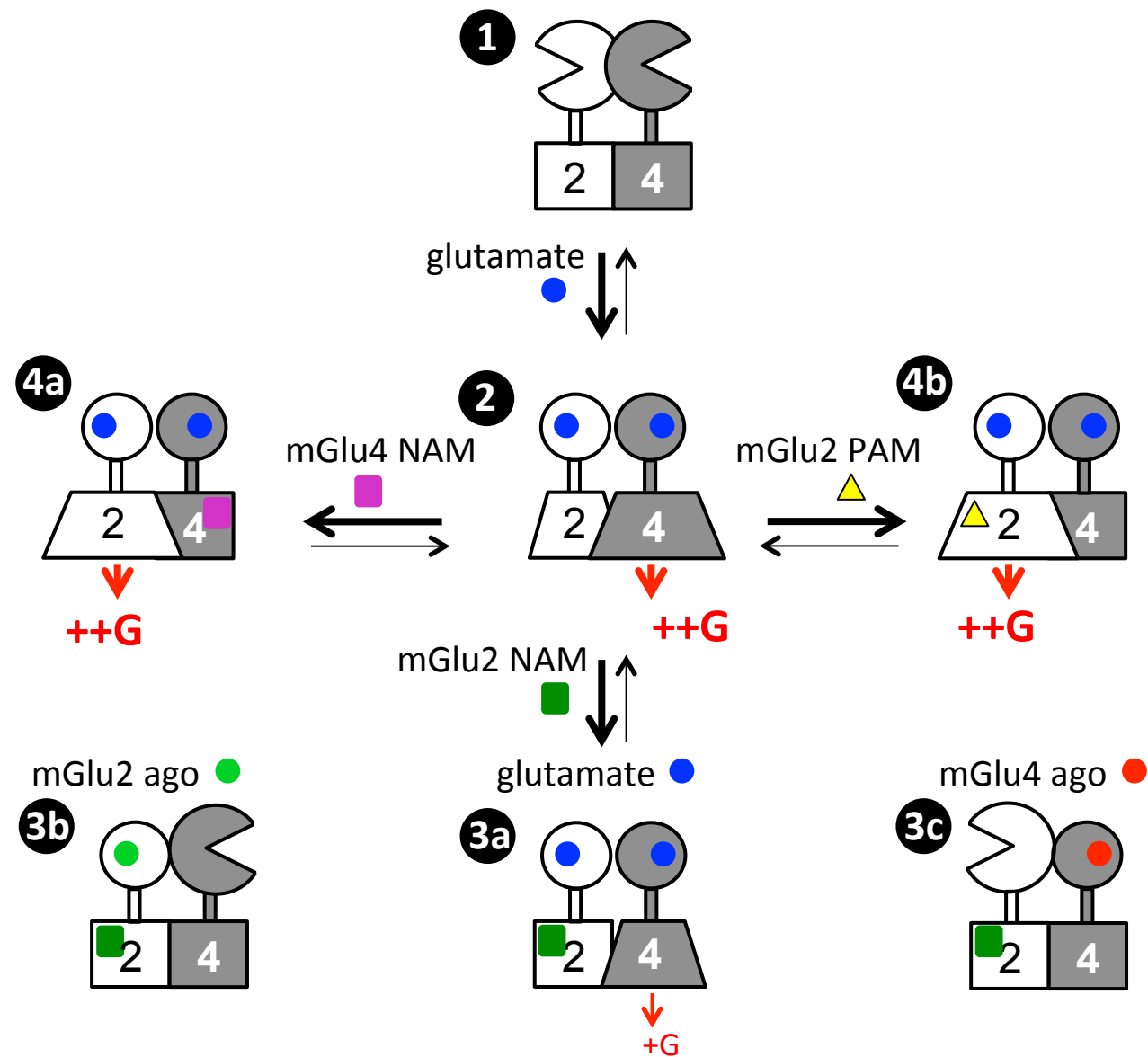


Figure 1- figure supplement 1

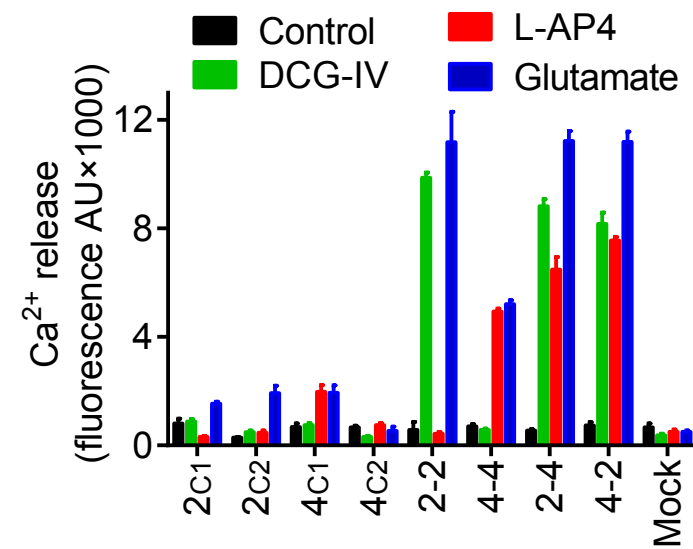


Figure 1- figure supplement 2

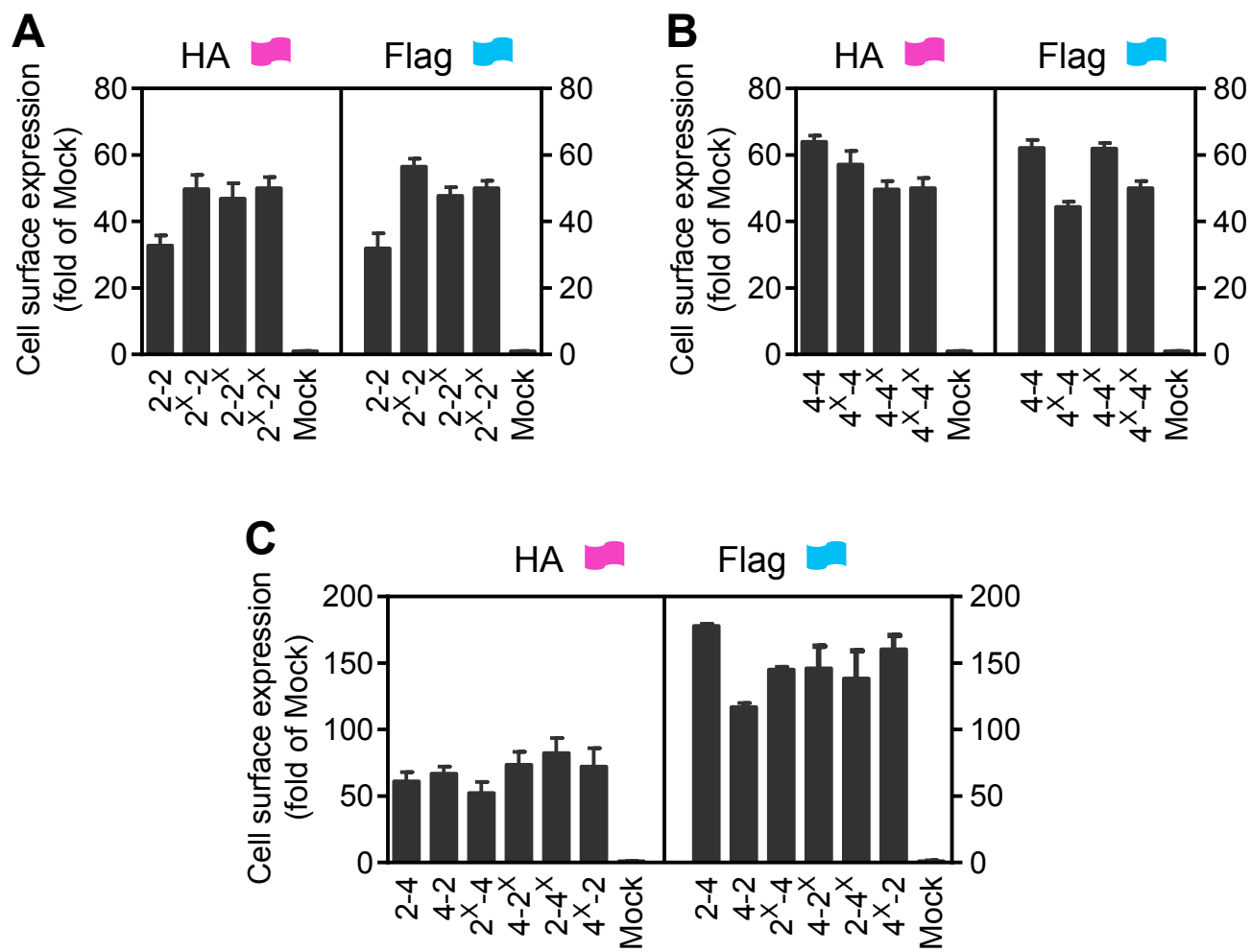


Figure 1- figure supplement 3

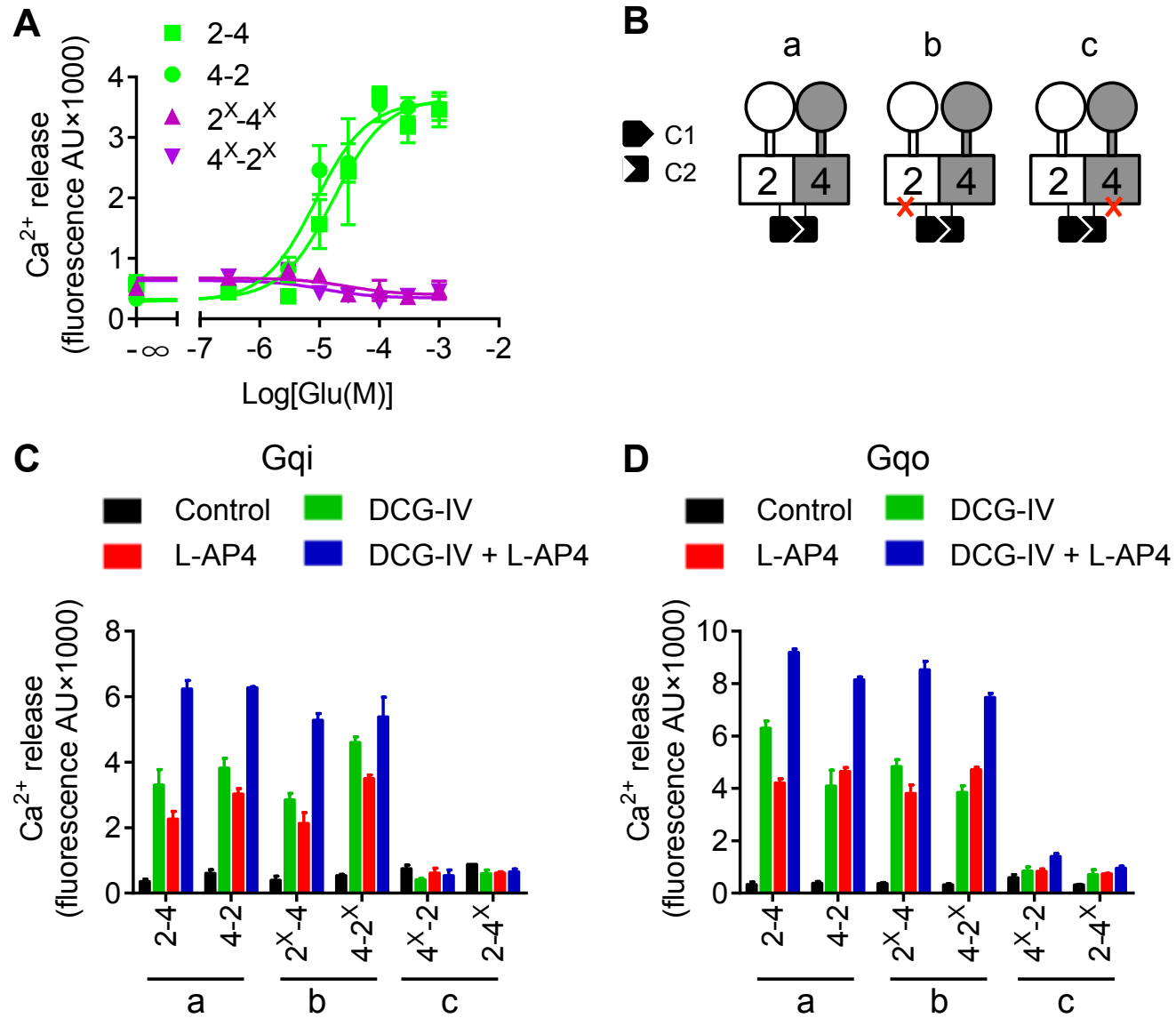


Figure 2- figure supplement 1

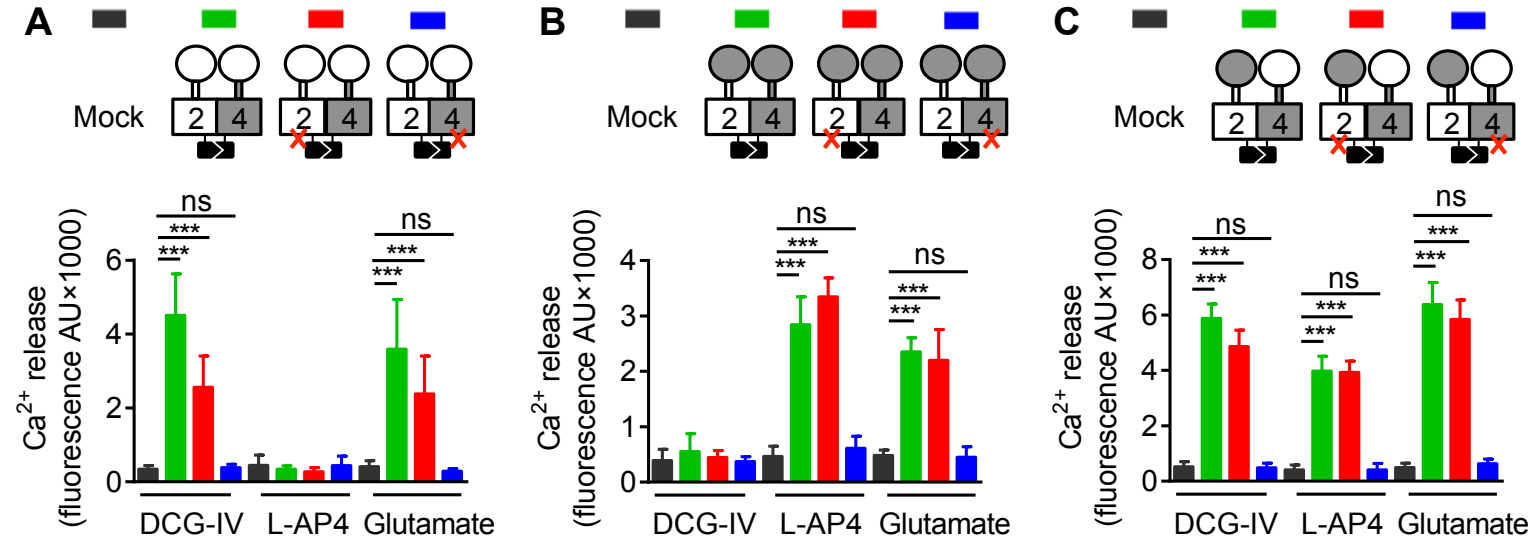


Figure 2- figure supplement 2

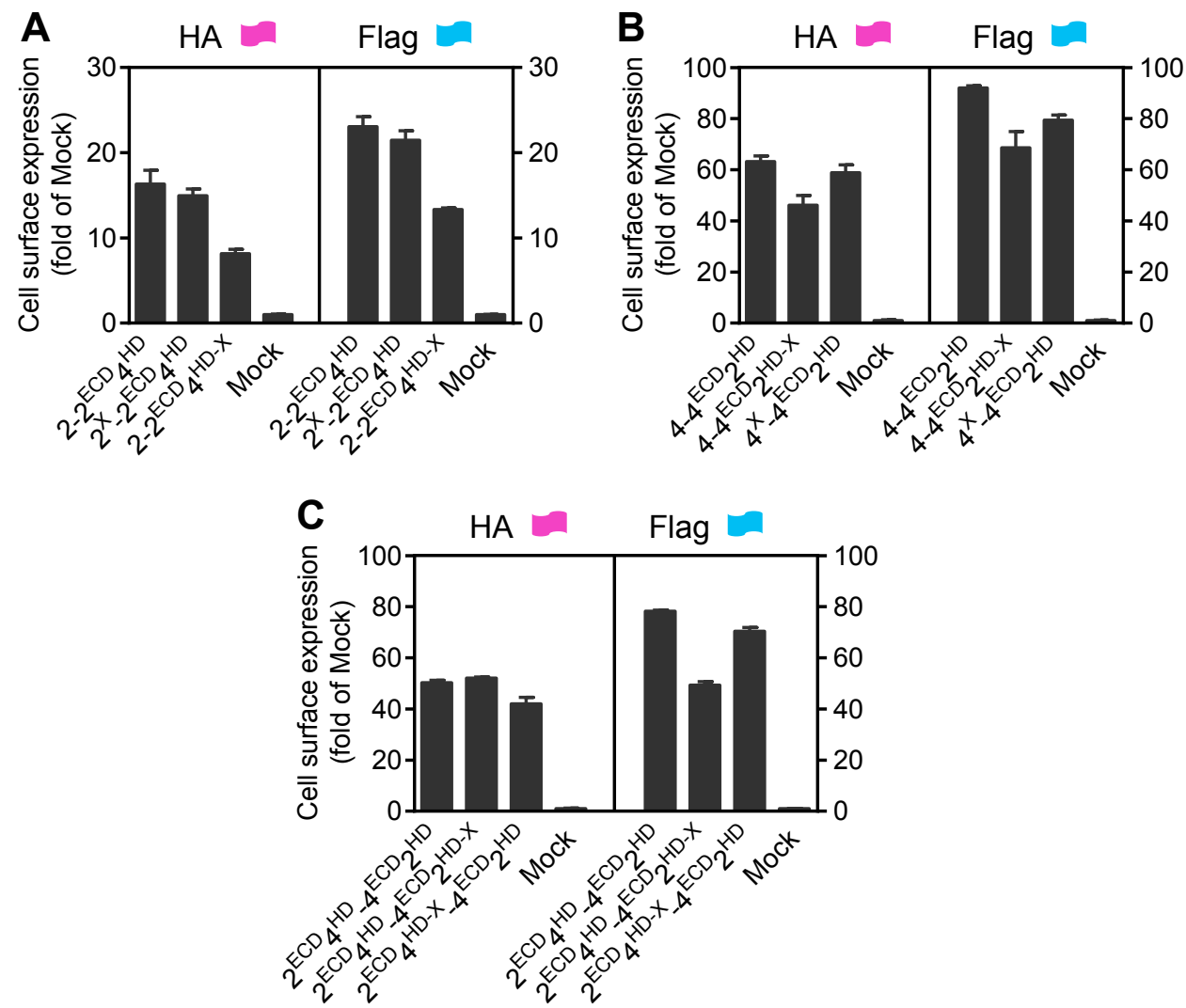


Figure 2- figure supplement 3

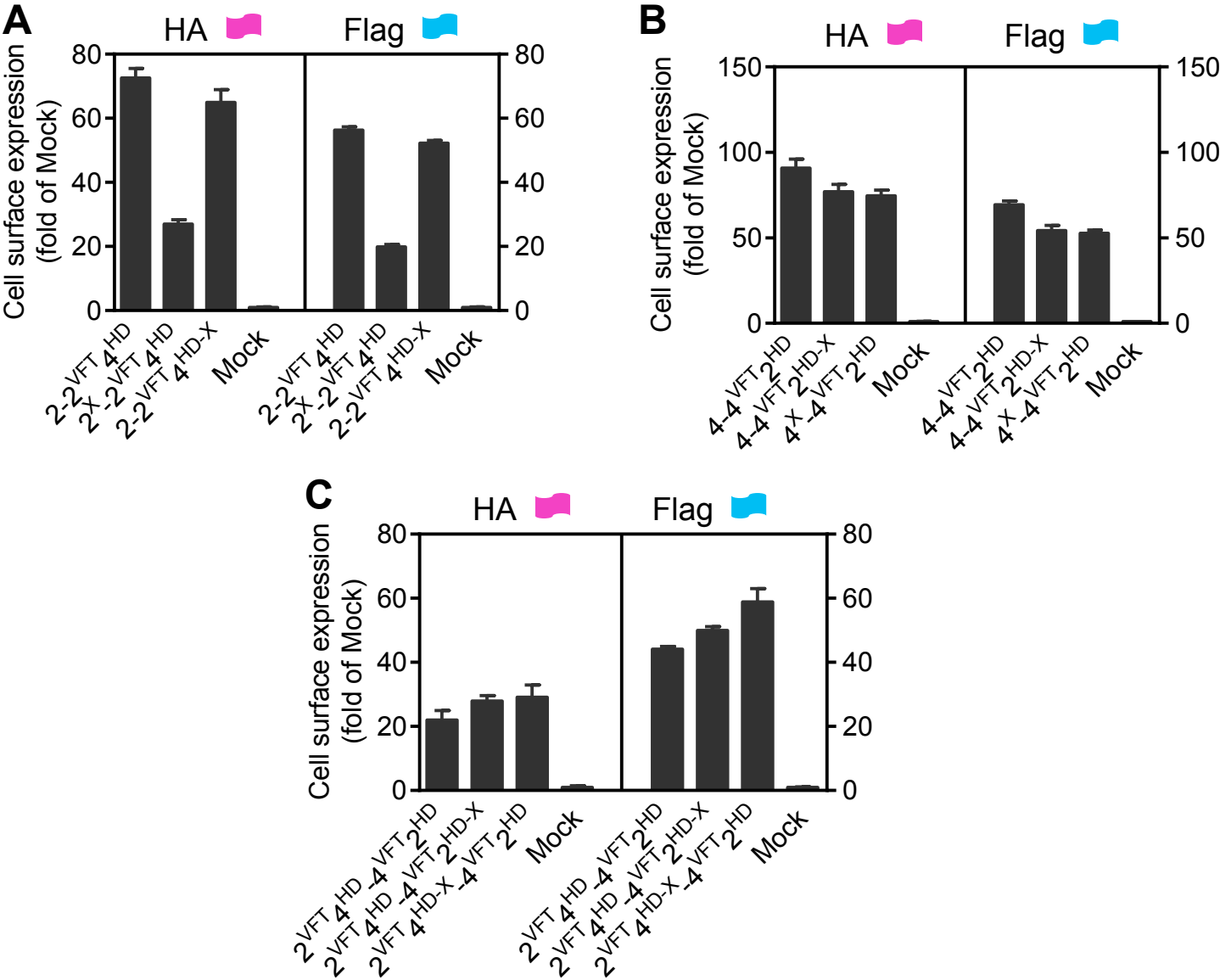


Figure 3 - figure supplement 1

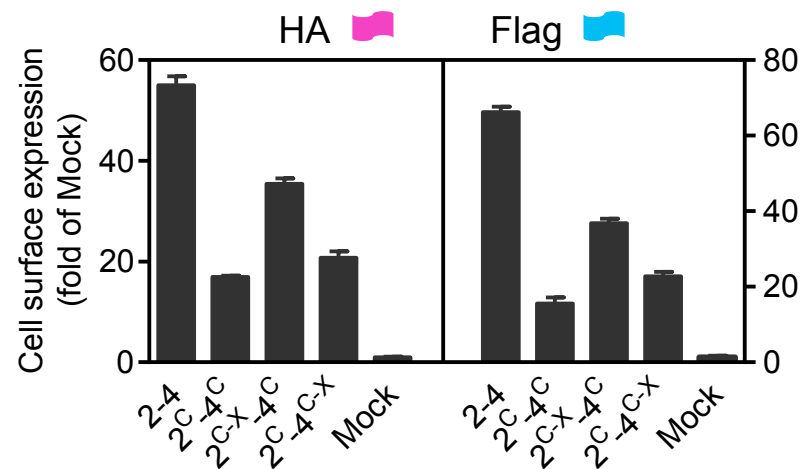


Figure 6- figure supplement 1

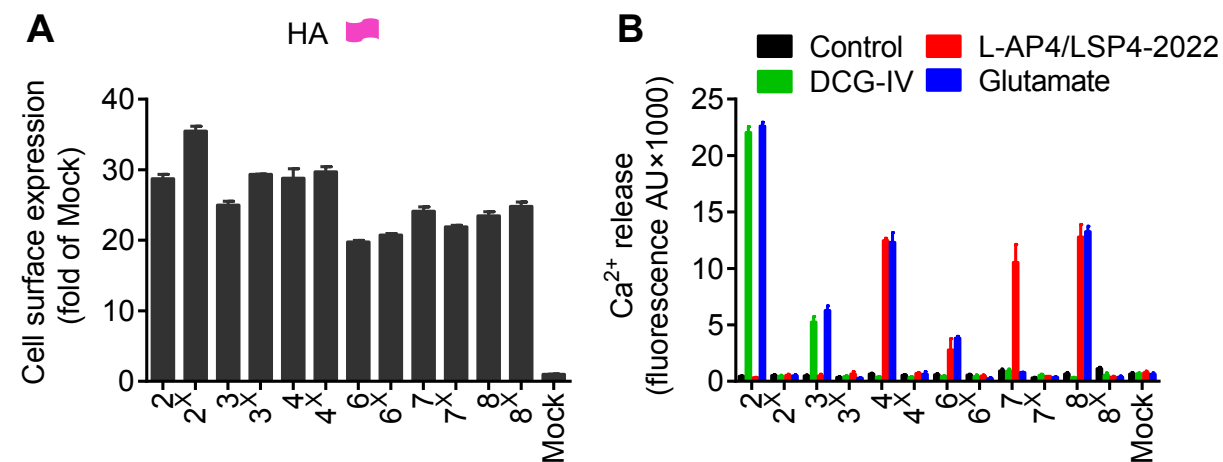


Figure 6- figure supplement 2

